# UNIVERSITÄTSKLINIKUM HAMBURG-EPPENDORF

Klinik für Kardiologie
Universitäres Herz- und Gefäßzentrum Hamburg

Direktor:
Prof. Dr. med. Stefan Blankenberg
Prof. Dr. med. Paulus Kirchhof


## CRIP1 in inflammatory diseases: A novel link between immune response and cardiovascular diseases

**Dissertation**

zur Erlangung des Grades eines Doktors der Medizin
an der Medizinischen Fakultät der Universität Hamburg.


vorgelegt von:

Teng Tong
aus Jiangsu, China



Hamburg 2022

**(wird von der Medizinischen Fakultät ausgefüllt)**

**Angenommen von der**
**Medizinischen Fakultät der Universität Hamburg am: 27.07.2022**

**Veröffentlicht mit Genehmigung der**
**Medizinischen Fakultät der Universität Hamburg.**

**Prüfungsausschuss, der/die Vorsitzende: Prof.Dr. Viacheslav Nikolaev**

**Prüfungsausschuss, zweite/r Gutachter/in: Prof.Dr. Tanja Zeller**

# Contents

# 1. Introduction

## 1.1 Definition and epidemiology of hypertension

Hypertension is defined as systolic blood pressure (SBP) values ≥ 140 mmHg and/or diastolic blood pressure (DBP) values ≥90 mmHg (Williams et al. 2018). Hypertension is a global health issue that has a significant economic impact. More than one billion individuals worldwide suffer from hypertension (Fisher and Curfman 2018), with more than 150 million in Central and Eastern Europe (Zhou et al. 2017). Hypertension affects more than 30% of the adult population (Mills et al. 2020), with worldwide age-specific prevalence rates of 24% for men and 20% for women (Zhou et al. 2017). Hypertension is prevalent worldwide, independent of income status, i.e., in low-, middle-, and high-income countries (Chow et al. 2013). The global prevalence of hypertension will continue to climb as populations age, adopt more sedentary lifestyles, and gain weight. By 2025, it is expected that the number of individuals with hypertension will have increased by 15–20%, bringing the total number of persons with hypertension to close to 1.5 billion (Kearney et al. 2005).

Hypertension is the leading cause of cardiovascular diseases and premature death worldwide (Forouzanfar et al. 2017, Mills et al. 2020). The incidence of various cardiovascular events, including myocardial infarction, heart failure, and peripheral artery disease, as well as stroke and end-stage renal disease, has an independent and continuous link with blood pressure (BP) (Lewington et al. 2002). There is also mounting evidence that hypertension has a relationship with an increased risk of atrial fibrillation (Lip et al. 2017), and that early blood pressure rises are linked to an increased risk of cognitive decline and dementia (Gottesman et al. 2017, Rovio et al. 2017).

Hypertension may be primary (or essential) or secondary. Primary hypertension is a type of high blood pressure that has no clearly identifiable cause but is thought to be linked to classical risk factors like genetics, poor diet, lack of exercise and obesity. It is by far the most common form of high blood pressure, affecting the majority of those who experience hypertension. Secondary hypertension is often diagnosed in the presence of an identifiable secondary cause. It accounts for approximately 5-10% of cases of hypertension (Rossier et al. 2017).

## 1.2 Pathophysiology mechanisms of hypertension

Hypertension is a multifactorial disease. Numerous evidence from experimental and clinical studies suggested that primary hypertension (essential hypertension) is caused by a complex interplay between environmental and genetic factors (Mills et al. 2016). Children of parents with primary hypertension are more likely to develop hypertension, and children of hypertensive families have a significantly higher blood

pressure response in sodium loading tests than children without a family history of hypertension (Raj 2011). Recent studies have identified abnormalities in somatic membrane ion transport in patients with primary hypertension and there is a strong genetic link (Aviv and Lasker 1992). Weight is an important factor in blood pressure, lowering weight can often lead to a reduction in blood pressure (Raj 2011, Llewellyn et al. 2016). Others, such as sympathetic nervous system (SNS) hyperexcitability, leads to increased blood pressure due to overproduction of epinephrine and norepinephrine (Ziegler and Milic 2017).

In pathophysiology, blood pressure levels depend primarily on cardiac output and total peripheral vascular resistance (Mayet and Hughes 2003). Any factor that causes an increase in cardiac output may lead to an increase in blood pressure, such as increased blood volume following water and sodium retention, increased myocardial contractility, or increased peripheral vascular resistance, such as constriction of peripheral arteries caused by neurological or endocrine factors. The former increases systolic blood pressure, while the latter increases diastolic blood pressure significantly.

There are also indirect factors that cause hypertension, including psychoneurological activity and some endocrine hormones that alter blood pressure through the direct determinants mentioned above, most notably the renin-angiotensin-aldosterone system (RAAS) (Saxena et al. 2018).

Reduced renal perfusion pressure caused by renal disorders, particularly renal vascular disorders, as well as reduced effective circulating blood volume and increased sympathetic activity, stimulate the secretion of large amounts of renin by periglomerular cells. Renin is a protein hydrolase that catalyzes the hydrolysis of angiotensinogen produced in the liver to angiotensin I (Ang I). Ang I is inactive and is converted to active angiotensin II (Ang II) by converting enzymes when it flows through various vascular beds, especially the pulmonary circulation. The latter has a strong vasoconstrictive effect, leading to an increase in blood pressure, and indirectly by stimulating the secretion of aldosterone from the adrenal cortex bulbous band, which causes the tubules to retain sodium and expand blood volume to raise blood pressure (Folkow et al. 1961, Bell and Madri 1990).

As the most widely used therapies for hypertension, angiotensin converting enzyme inhibitors (ACEI) interfere with the RASS by blocking the angiotensin-converting enzyme that converts Ang I to Ang II (Nasution 2006), while angiotensin receptor blockers (ARBs), also known as Ang II type 1 receptor antagonists, act as a treatment for high blood pressure by antagonizing receptor binding of Ang II on target organs (Li et al. 2014).

Secondary hypertension often has a clear cause. Increased blood pressure in acute glomerulonephritis and most substantial renal diseases is mostly associated with increased blood volume due to water and sodium retention, advanced glomerulosclerosis may also present with vasoconstrictive hyperreninemic hypertension (Johnson and Hunt 1982). Adrenal disorders cause hypertension through

the hormones they secrete (Laragh 1969). Primary aldosteronism produces hypertension as described above. In cortisolism, high levels of glucocorticoids lead to water and sodium retention and stimulate the production of angiotensin (Kelly et al. 1998). Pheochromocytoma secretes excessive amounts of epinephrine and norepinephrine, which raise systolic blood pressure by increasing myocardial contractility and heart rate and increasing cardiac output. Norepinephrine also produces a significant increase in both systolic and diastolic blood pressure due to peripheral vasoconstriction (Zuber et al. 2011). Aortic constriction causes upper limb hypertension due to mechanical obstruction and renal artery stenosis produces hyper-renin hypertension by affecting renal blood perfusion (Chiong et al. 2008). Central nervous system disorders such as tumors and encephalitis can occasionally cause severe hypertension, the pathogenesis of which is thought to be due to sympathetic excitation as the disease affects the stability of the autonomic nervous system, with increased cranial pressure as a possible precipitating factor (Mathias 1987, Chiong et al. 2008).

Hypertension is frequently confirmed to be associated with coronary heart disease. Several pathophysiologic mechanisms link these two diseases (Escobar 2002). Hypertension induces endothelial dysfunction, exacerbates the atherosclerotic process and it contributes to making the atherosclerotic plaque more unstable. Left ventricular hypertrophy, a common complication of hypertension, promotes a reduction in coronary reserve and increases myocardial oxygen demand, both mechanisms contributing to myocardial ischemia. It is important to emphasize that patients with hypertension have higher complications and mortality from myocardial infarction (Stamler et al. 1993, Escobar 2002). The common causes of primary and secondary hypertension are summarized in Table 1 below.

**Table 1. Common causes of hypertension**

| Classification | Causes |
|---|---|
| Primary hypertension | Age and sex (Mills et al. 2016) |
| | Obesity (Raj 2011, Llewellyn et al. 2016) |
| | Environmental factors e.g. sodium excess (Mills et al. 2016) |
| | Genetic factors (Raj 2011, Llewellyn et al. 2016) |
| | Sympathetic activation (Ziegler and Milic 2017) |
| | Activation of the renin-angiotensin-aldosterone system (Saxena et al. 2018) |
| Secondary hypertension | Renal parenchymal or renal vascular disease (Johnson and Hunt 1982) |
| | Endocrine diseases e.g. cortisolism and pheochromocytoma (Laragh 1969) |
| | Vascular diseases e.g. aortic or renal artery stenosis (Chiong et al. 2008) |
| | Central nervous system disorders (Mathias 1987, Chiong et al. 2008) |
| | Others (Escobar 2002) |

## 1.3 Inflammation, immunity and hypertension

Traditionally, hypertension has been thought to be a disorder of two systems that are involved in the regulation of salt-water balance and cardiovascular function: RAAS and the SNS. However, current therapies that aim to limit the influence of the RAAS or SNS on blood pressure fail in ~40% of cases (Cai and Calhoun 2017), which suggests that other mechanisms must be involved. During the past years, the immune system and inflammatory processes have emerged as key contributors to elevated blood pressure in several experimental animal and human models (Itani et al. 2016, Mikolajczyk et al. 2021, Drummond et al. 2019). New mechanisms associated with the pathogenesis and progression of hypertension have been discussed, of which the immune system and its activation may be critical. A relevant hypothesis is that immune cell accumulation in blood vessels, kidneys, heart and brain promote a chronic inflammatory response that disrupts the regulation of blood pressure in these organs, leading to hypertension (Norlander et al. 2018).

Almost every cell type involved in innate and adaptive immunity has been implicated in hypertension. Adaptive immune cells like T cells and B cells produce factors that promote or inhibit hypertension. Innate immune cells like macrophages, monocytes and dendritic cells (DCs) also produce cytokines and reactive oxygen species (ROS), which promote or inhibit hypertension (Drummond et al. 2019). The immune

mechanisms of hypertension are shown in Figure 1.

Chronic activation of the RAAS and SNS in non-immune mechanisms increases blood pressure and promotes mechanical and oxidative damage, thus results in cellular damage and an environment conducive to the chemical modification of proteins and ultimately the formation of danger-associated molecular patterns (DAMPs; such as mitochondrial DNA) and hypertension-specific neoantigens (Harrison et al. 2010). DAMPs (such as lipopolysaccharide) can also accumulate in the circulation and/or tissues as a result of intestinal dysbiosis or nutrition. DAMPs are detected by Toll-like receptors (TLRs) and NOD-, LRR- and pyrin domain-containing protein 3 (NLRP3) inflammasomes in monocytes, macrophages and dendritic cells (DCs), which produce pro-inflammatory cytokines (IL-1β and IL-18) and chemokines (CC-chemokine ligand 2 (CCL2) and CCL5) in response (Drummond et al. 2019).

Hypertension-specific antigens can be phagocytosed by DCs and presented to B cells and T cells within the spleen, which promotes the development of plasma cells and effector T cell subsets. Effector T cells migrate from sublymphoid organs to blood vessels, the heart and kidneys, where they attract and activate additional pro-inflammatory and profibrotic immune cells (such as monocytes and macrophages). Through the release of cytokines, they also have a direct impact on renal tubular salt transport and vascular resistance. Plasma cells produce IgG autoantibodies, which concentrate in blood vessels, kidneys and the heart, where they stimulate the receptors on macrophages and activate the complement system, promoting inflammation and fibrosis (Drummond et al. 2019).

The NLRP3 inflammasome in monocytes and DCs plays a key role in hypertension (Pasqua et al. 2018, Norlander et al. 2018). NLRP3 inflammasome can be activated by DAMPs or pathogen- associated molecular patterns (PAMPs) that lead to the maturation of IL-1β and IL-18 from inactive proforms. Recent studies have demonstrated the importance of the inflammasome to hypertension. In humans, circulating levels of IL-1β and IL-18 are increased in patients with hypertension (Rabkin 2009). Wang *et al.* (Wang et al. 2014) showed that hypertension is blunted in inflammasome-deficient $ASC^{-/-}$ and $NLRP3^{-/-}$ mice using a model of renin-dependent renovascular hypertension. Krishnan *et al* (Krishnan et al. 2016). demonstrated that $ASC^{-/-}$ mice are protected from renal inflammation, fibrosis, and elevated blood pressure induced by Deoxycorticosterone acetate (DOCA)-salt. The authors also demonstrated that a specific NLRP3 inhibitor reverses DOCA salt-induced hypertension, indicating a causal role for the inflammasome and its key cytokines, IL-1β and IL-18, in the development of hypertension.

A major goal of hypertension management is the prevention of cardiovascular diseases (CVD) and end-organ damage. It's becoming clear that inflammation within the target organs is responsible for a significant percentage of the vascular, renal, cardiac, and brain damage and dysfunction that comes with hypertension. Hypertension is also exacerbated by organ inflammation. Especially in the kidney,

immune cells infiltrate the kidney and release cytokines such as IL-1β, TNF-α, IFN-γ, and IL-17A. These mediators up-regulate sodium transporter expression and activity, causing sodium and water retention; damage kidney tissue, resulting in albuminuria and nephrinuria; alter renal vasculature, causing rarefaction and remodeling; and enhance ROS production within the kidney (Krebs et al. 2020, Norlander et al. 2018). All these findings highlight the role of the immune system as a potential therapeutic target for hypertension.

Despite a great deal of research into the immune mechanisms underlying hypertension, the immune system is highly interdependent and how these different cells and mediators interact in hypertension remains to be elucidated.

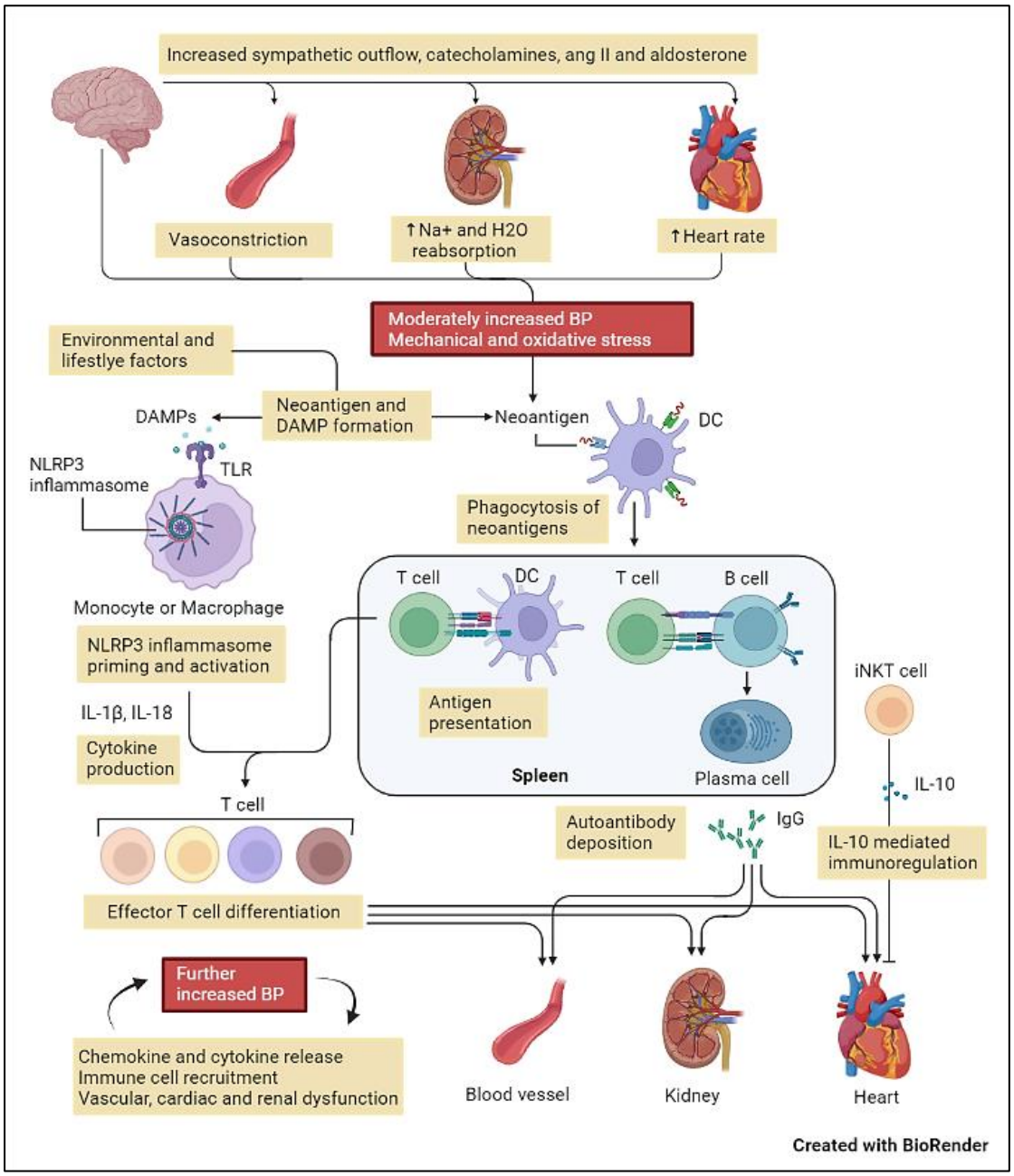


**Figure 1. The immune mechanisms of hypertension** (modified from Drummond *et al.*,

2019). Almost every cell type involved in innate and adaptive immunity has been implicated in hypertension. Immune cell accumulation in blood vessels, kidneys, heart and brain promote a chronic inflammatory response that disrupts the regulation of blood pressure in these organs, leading to hypertension, during which the NLRP3 inflammasome and its cytokines play a key role.

## 1.4 Cysteine-rich intestinal protein 1 (CRIP1) and hypertension

There is a substantial genetic heritability of 30% to 60% for hypertension (Levy et al. 2000). Large-scale genome-wide association studies on hypertension or BP traits have been published (Surendran et al. 2016, Ehret et al. 2016, Warren et al. 2017). Some of the identified genetic variants primarily associated with higher BP also confer an increased risk for coronary artery disease, consistent with a causal relationship of increased BP and coronary artery disease risk (Lieb et al. 2013, Warren et al. 2017). However, most genes near the identified genetic variants are not known to be functionally related to BP (Ehret et al. 2011).

In a large-scale population-based (including >4500 individuals) transcriptome analysis of human monocytes, Zeller *et al.* (Zeller et al. 2017) identified 8 candidate transcripts to be associated with blood pressure with *CRIP1* as the most relevant transcript. In this study, monocytic *CRIP1* expression levels were associated with long-term changes in blood pressure over 5 years, in response to blood pressure-lowering treatment and were related to the incident stroke. In a twin study, it was also shown that CRIP1 expression level was significantly associated with BP (Huang et al. 2018).

The study of Zeller *et al.* (Zeller et al. 2017) also revealed that the expression of *CRIP1* was highly associated with variants in the SH2B3/LNK locus. SH2B3 is a negative regulator of growth factors and cytokine signaling, and previous data have already implicated this locus as a master regulator involved in BP regulation (Ehret et al. 2011, Rotival et al. 2011, Rudemiller et al. 2015). A *Sh2b3*$^{-/-}$ knockout leads to markedly elevated BP in response to a low dose of Ang II (Huan et al. 2015). It is speculated that the effect of *SH2B3* on BP was mediated in part by *CRIP1* (Zeller et al. 2017).

These studies demonstrate the potential value of CRIP1 as a circulating marker of hypertension. However, the underlying mechanisms by how CRIP1 contribute to the pathogenesis of hypertension are not yet understood.

### 1.4.1 The structure and biological function of CRIP1

CRIP1 is a small molecular protein with a double tandem repeat zinc-finger motif and belongs to the LIM domain-containing protein family (Khoo et al. 1997). It was first

discovered and named in 1986 (Birkenmeier and Gordon 1986), and then many investigations have proved that CRIP1 plays an important role in zinc ion absorption and transport, maintenance of the luminal structure, and inflammatory immune response.

In 1986, Birkenmeier *et al.* screened a cDNA library from the small intestine of lactating to weaning rats and found an mRNA of 570 bp in length with highly variable expression. The fragment encodes 77 amino acids and has a relative molecular weight of 8.55 kDa, with 9% of the cysteine residues, hence the name cysteine-rich intestinal protein (CRIP) (Birkenmeier and Gordon 1986). CRIP1 has a small molecular weight, a simple structure with a double zinc finger structure-LIM domain, a few amino acid sequences at the C-terminus, and a lack of DNA-binding homology domain (Cai et al. 2017). The LIM domain was thought to play an important role in the involvement of CRIP protein in physiological processes such as development or immune defense (Kadrmas and Beckerle 2004, Schmeichel and Beckerle 1994).

It was found that CRIP1 transcripts were widely expressed in rodent tissues and cells such as small intestine, colon, spleen, brain, abdominal macrophages, and peripheral blood mononuclear cells (Birkenmeier and Gordon 1986), and its function is tissue-specific. CRIP1 is highly expressed in the small intestine and may play a role in regulating the transport of zinc ions, nutrient absorption, and growth and differentiation of intestinal epithelial cells (Khoo and Cousins 1994, Birkenmeier and Gordon 1986). In abdominal macrophages and spleen, CRIP1 is mainly involved in physiological processes such as the body's immune response (Khoo and Cousins 1994). Lanningham-Foster *et al.* (Lanningham-Foster et al. 2002) revealed that transgenic mice overexpressing CRIP1 showed an unbalanced immune response following lipopolysaccharide (LPS) treatment or influenza virus infection, favoring a Th2 response and showing a greater diarrhea incidence, cytokine dysregulation, and increased mortality than control mice. This suggests that CRIP1 does not directly mediate the immune response of the host, but plays an intermediate bridging or modifying role in its occurrence (Lanningham-Foster et al. 2002, Kadrmas and Beckerle 2004). In addition, CRIP1 was found to be highly expressed in the peripheral blood transcriptome of the elderly population, suggesting that this gene may be associated with the development of age-dependent diseases (Nakamura et al. 2012).

### 1.4.2 Association of CRIP1 with cardiovascular diseases

Recently, the link between CRIP1 and CVD and the immune system has received increasing attention. Zeller *et al.* found that the transcription level of CRIP1 is strongly correlated with changes in blood pressure, and is positively correlated with the risk of stroke (Zeller et al. 2017). The current studies imply many possible reasons for the close association of CRIP1 with blood pressure changes and CVDs.

CRIP1 expression was highly increased in the renin-expressing Juxtaglomerular cells, which are crucial for blood pressure regulation (Brunskill et al. 2011,

Castellanos-Rivera et al. 2015). Furthermore, it has been shown that a CRIP1 deletion in zebrafish larvae disturbs cardiac development and is lethal (Straubinger et al. 2017). CRIP1 is also highly expressed in immune cells, which suggests a correlation between CRIP1 and blood pressure management through the immune system. The inflammatory response and immune activation are benign responses that occur in the early stages of blood pressure elevation, but inflammatory factors are released in response to inflammation can contribute to the development of hypertension. CRIP1 protein is highly expressed in monocytes, macrophages and peripheral mononuclear cells and is upregulated by proinflammatory modulation in these cells (Hallquist et al. 1996). Lanningham-Foster *et al.* showed that CRIP1 overexpression in transgenic mice alters cytokine patterns and the immune response (Lanningham-Foster et al. 2002), demonstrating the contribution of CRIP1 in the inflammatory response. Schweigert *et al.* showed in a mouse hypertension model, that CRIP1 expression in splenic and circulating monocytes was significantly affected by pro-hypertensive hormone angiotensin II, indicating that CRIP1 may affect the interaction between the immune system and the pathogenesis of hypertension (Schweigert et al. 2021). The published information on the connection between CRIP1 and CVD is shown in Table 2.

There are many indications of immunological alterations in hypertension, but the exact molecular mechanisms of these changes are not clarified yet. CRIP1 may take part in the pathophysiology of hypertension by renal specific and immunoregulatory functions.

**Table 2. Published information on a connection between CRIP1 and CVD**

| Year | Findings |
|---|---|
| 2011 (Brunskill et al. 2011), 2015 (Castellanos-Rivera et al. 2015) | CRIP1 expression was highly increased in the renal cells which are crucial for blood pressure regulation |
| 2017 (Zeller et al. 2017) | The transcription level of CRIP1 is strongly correlated with changes in blood pressure |
| 2017 (Straubinger et al. 2017) | CRIP1 deletion in zebrafish larvae disturbs cardiac development, and significant enrichment of CRIP1 in murine hearts lacking CRP4 (CRIP2) |
| 2021 (Schweigert et al. 2021) | CRIP1-positive circulating and splenic monocytes play an important role in hypertension-related inflammatory processes through Ang II |

Several studies have confirmed the involvement of CRIP1 in the pathophysiology of CVD. Available evidence suggests that CRIP1 maybe take part in the development of hypertension and CVDs through renal specific and immunoregulatory functions.

## 1.5 Aims of this thesis

Based on our preliminary data that CRIP1 expression was strongly associated with blood pressure in the monocytic transcriptome-wide analysis (Zeller et al. 2017), and showed that CRIP1 was involved in inflammation in monocytes (Schweigert et al. 2021), this thesis aims to elucidate the role of CRIP1 in hypertension and CVDs related inflammatory processes using a human monocytic cell line and murine inflammation models.

The specific aims of this thesis are

Aim 1: Establish a stable CRIP1-downregulated cell model via shRNA in the monocytic-like cell line THP-1.

Aim 2: Investigate the role of CRIP1 for cell cytotoxicity and viability as well as alterations in cytokine and chemokines known to be involved in CVDs upon induction of inflammation.

Aim 3: Investigate expression of *Crip1* and its correlations with inflammatory mediators in established mouse models of inflammation and kidney disease.

# 2. Materials and Methods

## 2.1 Materials

### 2.1.1 Laboratory consumables

| | |
|---|---|
| Cell culture flasks | Sarstedt AG & Co. KG |
| 6, 12, 96 – well suspension cell culture plate | Sarstedt AG & Co. KG |
| 6, 12, 96 – well adherent cell culture plate | Sarstedt AG & Co. KG |
| Serological pipettes (1ml) | Cellstar®, Greiner Bio-GmbH |
| Serological pipettes (5ml, 10ml, 25ml) | Sarstedt AG & Co. KG |
| Tubes (15ml, 50ml) | Eppendorf AG |
| Reaction tubes (1.5ml, 2ml) | Eppendorf AG |
| Pipette filter tips (10 µl, 20 µl, 100 µl, 200 µl, 1000 µl) | Biosphere®, Sarstedt AG & Co. KG |
| 384-well PCR plates | Sarstedt AG & Co. KG |
| Optical adhesive cover | Applied Biosystems®, Thermo Fischer Scientific |
| 96-well UV transparent tissue culture plates | Cellstar®, Greiner Bio-GmbH |
| Pipet tips for gel loading (1–200 µl) | BioRad |
| Transfer Pack Midi Format, 0.2 µm Nitrocellulose, Trans-Blot Turbo (immunoblot) | BioRad |
| 96-well opaque-walled tissue culture plates, white | Microtiter™, Thermo Fischer Scientific |
| 96-well opaque-walled tissue culture plates, black | Microtiter™, Thermo Fischer Scientific |
| Cell brushes | Sarstedt AG & Co. KG |

### 2.1.2 Chemicals and reagents

| | |
|---|---|
| RPMI 1640, w/o: L-glutamine, w: 2.0 g/L NaHCO3, very low endotoxin | PAN™, Biotech |
| Penicillin 100U/ml, Streptomycin 100 µg/ml (Pen/Strep) | Sigma |
| β-Mercaptoethanol for molecular biology | Gibco™, Thermo Fischer Scientific |
| Trypan Blue | Abcam |
| Phosphate Buffered Saline 1X (PBS) | Gibco™, Thermo Fischer Scientific |
| Fetal Bovine Serum (Heat inactivated) | Gibco™, Thermo Fischer Scientific |
| Puromycin | Santa Cruz Biotechnology |

| | |
|---|---|
| Plasmid Transfection Medium | Santa Cruz Biotechnology |
| Lipofectamin® 2000 | Invitrogen™, Thermo Fischer Scientific |
| DNase/RNase Free Water | Invitrogen™, Thermo Fischer Scientific |
| Ethanol 100% (v/v) for molecular biology | Applichem |
| Phorbol 12-myristate 13-acetate (PMA) | Sigma |
| Lipopolysaccharide (LPS) | Cell Signaling Technology |
| Adenosine Triphosphate (ATP) | Sigma |
| Phosphatase Inhibitor Cocktail | Sigma |
| Protease Inhibitor Cocktail | Sigma |
| RIPA Lysis and Extraction Buffer | Pierce®, Thermo Fischer Scientific |
| Ammonium Persulfate (APS) | Sigma |
| Bromophenol blue | Roth |
| Glycerol | AppliChem GmbH |
| Sodium Dodecyl Sulfate in pellets (SDS) | Roth |
| Trizma Base | Sigma |
| Glycin | Roth |
| Methanol | Sigma |
| Powdered Milk | Roth |
| Albumin Bovine Fraction V, pH 7.0 (BSA) | Serva |
| NaCl | Roth |
| HCl (for pH) | Merck |
| TEMED: N, N, N', N' – tetramethyl ethylenediamine | Sigma |
| Tween® 20 | Sigma-Aldrich |

### 2.1.3 Plasmids

| | |
|---|---|
| Control shRNA Plasmid-A: sc-108060 | Santa Cruz Biotechnology |
| CRIP1 shRNA Plasmid (h): sc-92384-SH | Santa Cruz Biotechnology |

### 2.1.4 Cell line and mouse strain

| | |
|---|---|
| THP-1 Cell Line | TIB-202™, American Type Culture Collection ® |
| C57BL/6 Mice | mod. Krebs *et al.*, 2020 (Krebs et al. 2020) |

### 2.1.5 Antibodies and protein markers

| | |
|---|---|
| GAPDH (14C10) Rabbit mAb, (HRP Conjugate) , # 3683s, 1:3000 dilution | Cell Signaling Technology |
| Anti-CRIP1 antibody [EPR14345], Host Rabbit, Monoclonal, # ab183029, 1:50000 dilution | Abcam |
| HRP Goat Anti-Rabbit IgG Antibody (Peroxidase),# PI-1000-1, 1:10000 dilution | Vector Laboratories, Maravai Life Science |
| Prestained Protein Ladder, # 26619 | PageRuler$^{TM}$ Plus, Thermo Fischer Scientific |

### 2.1.6 Buffers and solutions

| | |
|---|---|
| 10% Ammonium persulfate (APS) | 10% (w/v) dissolved in $dH_2O$ |
| Antibody Dilution Buffer | 1 or 5% (w/v) BSA dissolved in TBST |
| Blocking Buffer | 5% (w/v) Non-fat Dry Milk dissolved in Tris Buffered Saline (TBS) |
| Loading Buffer: Laemmli Buffer (6x) | 0.375M Tris pH 6.8,<br>12% SDS,<br>60% Glycerol,<br>2.5% ß-Mercaptoethanol,<br>0.06% Bromophenol blue |
| 10% Sodium Dodecyl Sulfate (SDS) | 10%(w/v) Sodium Dodecyl Sulfate dissolved in $dH_2O$ |
| SDS-Running buffer | 25 mM Tris<br>192 mM Glycine<br>0.1% (w/v) SDS |
| Transfer Buffer | 25 mM Tris<br>192 mM Glycine<br>20% Methanol |
| Tris Buffered Saline (TBS) | 50 mM Tris<br>1.5 M NaCl,<br>(pH 7.6 with HCl) |
| Tris Buffered Saline with Tween® 20 (TBST) | TBS with 0.05% Tween 20 |
| Cryoconservation Solution (freeze medium) | 95%FCS + 5%Dimethyl Sulfoxide |

### 2.1.7 Molecular biology kits

| | |
|---|---|
| RNeasy Mini Kit | QIAGEN GmbH |
| RNase Free DNase Set | QIAGEN GmbH |
| High-Capacity cDNA Reverse Transcription Kit | Applied Biosystems™, Thermo |

| | |
|---|---|
| | Fischer Scientific |
| TaqMan™ Gene Expression Master Mix | Applied Biosystems™, Thermo Fischer Scientific |
| TaqMan Gene Expression Assays | Applied Biosystems™, Thermo Fischer Scientific |
| Pierce BCA Protein Assay Kit | Thermo Scientific |
| Clarity™ Western ECL Blotting Substrate | BioRad |
| SuperSignal™ West Femto Substrate | Thermo Scientific |
| RealTime-Glo™ MT Cell Viability Assay | Promega |
| CellTox™ Green Cytotoxicity Assay | Promega |
| Lumit™ IL-1β Human Immunoassay | Promega |
| Lumit™ Immunoassay Cellular Systems | Promega |
| Human IL-18 ELISA Kit | MBL Life Sciences Company |

### 2.1.8 Equipment

| | |
|---|---|
| Centrifuge Functional Line 400R | Heraeus Instruments GmbH |
| Centrifuge Heraeus Megafuge 16R | Thermo Scientific |
| Pipettes Research® / Reference® | Eppendorf AG |
| Multipette E3 | Eppendorf AG |
| Pipette Pipetus® | Hirschmann Laborgeraete GmbH & Co. KG |
| Thermomixer 5436 | Eppendorf |
| Vortex mixer Vortex-Genie 2 | Scientific Industries, Inc |
| Mini Centrifuge Fisherbrand™ | Fisher Scientific GmbH |
| Precision Scale AZ 212 M-Power | Sartorius |
| Digital Tube Roller SRT6D | Stuart, Cole-Parmer GmbH |
| Water Bath | Gesellschaft für Labortechnik GmbH |
| Microscope | Leica Microsystems, Cambridge Ltd. |
| Microscope | ZEISS ApoTome |
| $CO_2$ Incubators Heracell™ | Thermo Scientific |
| Biological Safety Cabinet, HeraSafe KS-12 Class II A2 Laminar Flow Biohazard Hood | Thermo Scientific |
| Hemocytometer (Neubauer chamber) | Glaswarenfabrik Karl Hecht GmbH & Co KG |
| Mr. Frosty™ Freezing Container | Thermo Scientific |
| Microplate Reader Infinite 200/200Pro | Magellan, Tecan Diagnostics |
| NanoDrop™ 2000/2000c Spectrophotometer | NanoDrop Technologies Inc. USA, Thermo Scientific |
| Thermal Cycler, GeneAmp® PCR System 9700 | Applied Biosystems™, Thermo Scientific |

| | |
|---|---|
| QuantStudio 7 Flex Real-Time PCR System | Applied Biosystems™, Thermo Scientific |
| Immunoblot Apparatus Mini-PROTEAN Tetra Cell | BioRad |
| Trans-Blot Turbo Transfer System | BioRad |
| Immunoblot Imaging System Fusion SOLO S | Vilber Lourmat |
| GloMax® Discover Microplate Reader | Promega |

### 2.1.9 Software

| | |
|---|---|
| QuantStudio™ Real-Time PCR Software v1.3 | Thermo Scientific |
| VisionCapt V 16.11a | Vilber Lourmat |
| Magellan V 7.2 | Tecan Austria GmbH |
| GraphPad Prism 8 | GraphPad Software |

## 2.2 Methods

### 2.2.1 Cell culture

The cell line used in this thesis was THP-1, obtained from American Type Culture Collection (ATCC). THP-1 is a human monocytic leukemia cell line that was established in 1980 by Tsuchiya *et al* (Tsuchiya et al. 1980). It was derived from the blood of a patient with acute monocytic leukemia. THP-1 cells resemble primary monocytes and macrophages in morphology and differentiation properties. THP-1 cell shows a large, round single-cell morphology and expresses distinct monocytic markers (Verhoeckx et al. 2015). This cell line has become a common model to estimate modulation of monocyte and macrophage activities (Chanput et al. 2014).

#### 2.2.1.1 Subculture of THP1 cell line

THP-1 cells were grown in 75cm$^2$ flasks in RPMI 1640 medium (PAN Biotech, P04-17525) supplemented with 10% fetal bovine serum (FBS, Gibco), 1% Penicillin /Streptomycin (Pen/Strep, penicillin 100U/ml and streptomycin100µg/ml, Sigma) and 0.05 mM ß-mercaptoethanol (Gibco). Between passaging, cells were grown in an incubator at 37 ℃ in an atmosphere of 5% $CO_2$ in the air. Following the fresh medium was pre-warmed to 37 ℃ in a water bath, the medium was exchanged, and cells were split in a 1:3-5 ratio at least twice per week.

#### 2.2.1.2 Cell counting

To quantify the number of cells for further experiments and to distinguish the living cell from the dead ones, cells were placed in the hemocytometer (Neubauer counting chamber) and incubated with Trypan blue dye. Dead cells absorb the dye and appear blue during the microscopic examination while living cells show up in a light color

during microscopic examination. The thick glass chambers are divided into sections of the calibrated area and depth. The number of cells in the four 1-mm large corner squares (labeled “L”) was counted and the cell concentration was calculated using the following formula. (Figure 2)

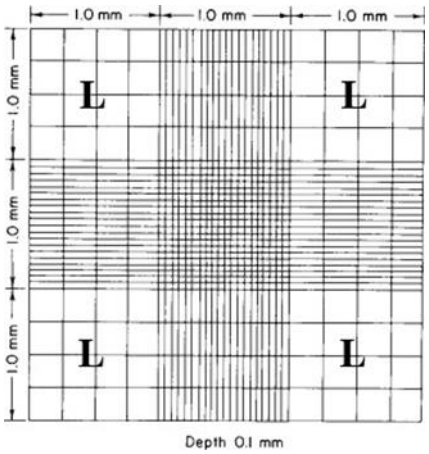


**Figure 2. Line drawing of the ruling of Neubauer counting chamber.** Chamber units are 1 mm with a depth of 0.1 mm. The cell number per ml was counted using the following formula and prepared for seeding in desired cell concentration according to the counted cell number.

$$\text{Cell number in ml}^{-1} = \frac{\text{Cell number in 4 large squares (L)}}{4} \times 10^4 \times \text{ml}^{-1}$$

#### 2.2.1.3 Freezing cells

Cells were counted and a total volume of 10 million cells was transferred to a falcon tube and centrifuged at the speed of 1800 rpm for 5 min. After centrifugation, the supernatant was removed, and the cell pellet was dissolved in 1 ml freeze medium and transferred to a cryo-tube after resuspension. The cryo-tube was placed for at least 24h in a Mr. Frosty™ freezing container at -80 ℃ for slow freezing. Then the frozen cells were transferred to liquid nitrogen (vapor phase) for long-term preservation.

#### 2.2.1.4 Thawing cells

For thawing cells, the frozen cells stored in liquid nitrogen were thawed quickly in the water bath then immediately transferred to a falcon tube containing warm medium and centrifuged at 1800 rpm for 5 min. The supernatant was removed and the pellet was dissolved in 10-20 ml culture medium, which was then transferred to a new culture flask.

### 2.2.2 ShRNA plasmid transfection and single clone selection

Small/short hairpin RNA (shRNA) was used to stably downregulate CRIP1 in the target cell line THP-1. ShRNA plasmids are normally supplied as a pool consisting of three to five lentiviral vector plasmids. After shRNA transfection, stably transfected cells expressing shRNA will be selected by adding puromycin.

#### 2.2.2.1 Transfection with Lipofectamine™ 2000

THP-1 cells were stably transfected with control shRNA plasmid (sc-108060) and CRIP1 shRNA plasmid (sc-92384-SH) mixed with transfection reagent (Lipofectamine™ 2000) according to manufacturer's protocol. In brief, cells were seeded in a 6-well tissue culture plate and grew to a 50–70% confluency in an antibiotic-free normal growth medium supplemented with FBS. Before transfection, cells were washed twice with plasmid transfection medium and resuspended in 800 µl plasmid transfection medium each well. For transfection, 1 µg (10 µl) of resuspended shRNA Plasmid DNA (either Control or CRIP1) and 3 µl of Lipofectamine™ 2000 were diluted into 187 µl plasmid transfection medium. After that, the shRNA plasmid and the transfection reagent were mixed gently by pipetting the solution up and down and then incubated for 30 min at room temperature. The ratio of shRNA Plasmid DNA and Lipofectamine™ 2000 transfection reagent was 1 µg:3 µl in this mixture. Then the 200 µl mixture was dropwise to each well, covering the entire layer and gently mixed by swirling the plate. The cells were incubated at 37 ℃ in a 5% $CO_2$ incubator for 6 h. After incubation, 1 ml of 2x normal growth medium (RPMI 1640 medium containing double concentration of FBS and Pen/Strep) was added into each well, and then incubated for an additional 24 hours.

#### 2.2.2.2 Transfected cell selection

The cells successfully integrated the shRNA sequence will get puromycin resistance. Puromycin is an aminonucleoside antibiotic produced by the bacterium Streptomyces alboniger. It inhibits protein synthesis by disrupting peptide transfer on ribosomes causing premature chain termination during translation. It is a potent translational inhibitor in both prokaryotic and eukaryotic cells. Resistance to puromycin is conferred by the puromycin N-acetyl-transferase gene (pac) from Streptomyces. Adherent mammalian cells are sensitive to concentrations of 2 to 5 µg/ml, while cells in suspension are sensitive to concentrations as low as 0.5 to 2 µg/ml. Puromycin-resistant stable mammalian cell lines can be generated in less than one week.

To determine the lowest concentration that kills 100% of the normal (untransfected) THP-1 cells, 2 x 10^5 healthy cells were seeded in a 6-well tissue culture plate with 2 ml of growth medium containing increasing concentrations of puromycin. (i.e., 0, 1.0, 2.5, 5.0, 7.5, and 10.0 µg/ml). Then cells were monitored daily to observe the percentage of surviving cells. The minimum antibiotic concentration to use is the lowest concentration that kills 100% of the cells in 3-5 days. For the THP-1 cell line, the appropriate concentration for puromycin selection was 1 µg /ml.

To select transfected cells, the transfection medium was aspirated from each well 48 hours post-transfection, and replaced with fresh medium containing puromycin. Every 2-3 days, aspirate and replace with freshly prepared selective medium.

#### 2.2.2.3 Single clone sorting

After selection steps, the living cells were all transfected with either control shRNA

plasmid or CRIP1 shRNA plasmid. The transfected cells were collected in a 1.5 ml tube and then diluted to 1 living cell per well in a 96-well plate in fresh growth medium using a cell sorter. After one week, the growing single-clone populations were transferred to a 24-well plate, and then later transferred to flasks for expanded culture. All the transfected clones were always cultivated in growth medium containing puromycin.

When the cells grew over the entire flask, as many clones as possible were frozen. CRIP1 expression in the single-clone cell populations was analyzed via qPCR and immunoblot analysis. Specifically, shCRIP1 plasmid transfected single-clone cell population with the lowest expression of CRIP1 was chosen for further experiments.

## 2.2.3 Stimulation and harvest cells

### 2.2.3.1 Cell stimulation

The day before the conduction of a stimulation experiment, THP-1 cells were seeded in 12-well or 6-well plates at a density of $5x10^5$/ml in fresh medium and incubated overnight at 37 ℃ in an atmosphere of 5% $CO_2$ in the air. In the CRIP1 knockdown cells compounds known to induce inflammation were used in this study (see table 3). Chemicals or compounds were prepared as stock solutions (except ATP) and stored according to the manufacturer's instructions.

Cells were stimulated with corresponding reagents prepared freshly before starting the experiment. After each stimulation step, plates were placed into the incubator at 37 ℃ in an atmosphere of 5% $CO_2$ in the air. Cells were harvested at specific time points.

**Table 3. Stimulation experiment implementation**

| Stimulation compounds | Concentration and storage of stock solution | Concentration of stimulation | Reagent used as control | Timepoints |
|---|---|---|---|---|
| PMA | 1 mg/ml in DMSO, -20 ℃ | 50 ng/ml | DMSO | 48 h |
| LPS | 1 mg/ml in PBS, -80 ℃ | 1 µg/ml | PBS | 3 h |
| ATP | Store as powder at -20 ℃, Dissolved 100 mM in $H_2O$ freshly | 5 mM | $H_2O$ | 30 min |

### 2.2.3.2 Harvesting cells and supernatant

To harvest the cells, suspension from each well was put in a tube and centrifuged 400x g for 5-10 min at 4 ℃. The supernatant was transferred to a new tube, centrifugated again at 13000 rpm at 4 ℃ for 30 min and frozen out the supernatant. The cell pellet was washed with 1x PBS and centrifugated 400x g for 10 min at 4 ℃. The supernatant was discarded, and the pellet was resuspended in the corresponding

buffers for protein or RNA analysis.

## 2.2.4 Real-Time PCR (RT-PCR) gene expression analysis

### 2.2.4.1 RNA isolation

Nucleic acids are negatively charged molecules due to the phosphate groups (PO3-) that are capable of being attracted to polar solvents like water. RNA and DNA precipitate out in the presence of salts and ethanol. RNA isolation kits exploit the properties of nucleic acids to extract purified RNA from cells and tissues. RNeasy® Mini Kit (QIAGEN) was used for RNA extraction. All samples were extracted according to the manufacturer's instructions.

Cell pellet for RNA isolation was added with 350 µl RLT buffer and stored at -80 ℃ in 1.5 ml tubes. For RNA isolation, 350 µl 70% ethanol was added into each tube after thawing and mixed by pipetting. The total volume of 700 µl was transferred to an RNeasy spin column and centrifuged for 8000x g for 30 s. The flow-through was discarded and the column was washed with Buffer RW1. DNase treatment was followed to remove DNA from the column. Then, the column was washed, centrifuged and RNA was eluted by adding 30-50 µl of RNase-free water into the column. The concentration and quality of total RNA were measured using NanoDrop.

### 2.2.4.2 Reverse transcription mRNA – Synthesis of complementary DNA (cDNA)

An mRNA molecule is free from introns and represents the amount of the gene that would be transcribed and translated into proteins. cDNA is synthesized from mRNA template in a reaction catalyzed by the enzymes reverse transcriptase and DNA polymerase. A poly-(A) tail, which is used as a primer site, helps in differentiating between mRNA, tRNA and rRNA in the cells. Reverse Transcriptases (RTs) synthesize the first strand of cDNA using the mRNA template and a short primer of oligo deoxy-thymidine nucleotides (oligo-dT). This oligo-dT is complementary to the 3' poly-(A) end of the RNA. RTs also use an RNase H function that degrades the RNA part of the hybrid. After this, only a single stranded cDNA molecule is present, and from this, a double stranded DNA is created by DNA polymerase.

All the RNA samples were normalized to 50 ng/µl in micro-amp 8-tube strips. The 2x Reverse Transcription master mix was prepared using the High Capacity cDNA Reverse Transcription kit (Table 4). The RNA and master mix were mixed in a 1:1 dilution. After incubation of 10 min, the samples were subjected to a cycle in the thermal-cycler with the conditions listed in Table 5. The final step was to dilute the cDNA sample at 1:10 with double distilled water to provide the end concentration of cDNA to 5 ng/µl. The samples were then frozen at -20 ℃ for longer periods and thawed when used for TaqMan analysis.

**Table 4. Contents and specifications for Master Mix preparation for 1 reaction**

| Product | Concentration | Final Concentration | Volume |
|---|---|---|---|
| RNA Template | 50 ng | 5 ng | 10 µl |
| RT Buffer | 10x | 1x | 2 µl |
| RT Random Primers | 10x | 1x | 2 µl |
| dNTP Mix | 100 mM | 4 mM | 0.8 µl |
| MultiScribe Reverse Transcriptase | 50 U/µl | 2.5 U/µl | 1 µl |
| RNase Free Water | - | | 4.2 µl |
| Total Volume of Reaction | | | 20 µl |

**Table 5. cDNA synthesis-cycler program**

| Step | Temperature | Time |
|---|---|---|
| Primer Annealing | 25 ℃ | 10 min |
| cDNA synthesis | 37 ℃ | 120 min |
| Inactivation of enzyme | 85 ℃ | 5 min |
| Hold | 4 ℃ | ∞ |

### 2.2.4.3 TaqMan Real-Time PCR (RT-PCR)

TaqMan RT-PCR is optimal for the detection and quantification of RNAs, especially with low abundance in a sample. TaqMan utilizes the simple 5´–3´ endonuclease activity of Taq polymerase to amplify the target gene in the cDNA sample by extending the primers on the template strand in a 3´-5´direction. The TaqMan probe is a hydrolysis probe that consists of two labels, one fluorescent at the 5'-end and a quencher at the 3'-end coupled with a minor groove binder, which helps quantify the amplified product via Fluorescent Resonance Energy Transfer (FRET).

The cDNA templates were thawed and kept on ice. 384-well plates were used for the TaqMan analysis in the Applied Biosystems™ QuantStudio 7 Flex Real-Time PCR System. 1 µl of cDNA template was added to 9 µl of Master Mix (Table 6) to the wells according to a pre-defined layout, the plate was covered with an optical adhesive cover and centrifuged. The cycler program was set up (Table 7) onto the QuantStudio™ Real-Time PCR System. All gene expression assays used in this thesis were listed in Table 8. For THP-1 cells, *GAPDH* was used as the housekeeper, and for murine samples, the geometrical mean of *Actb/Hprt* was used as the housekeeper.

**Table 6. Preparation of TaqMan gene expression master mix per reaction**

| Component | Concentration | Final Concentration | Volume |
|---|---|---|---|
| TaqMan™ Gene Expression Master Mix | 2x | 1x | 5 µl |
| TaqMan Gene Expression Assay | 20x | 1x | 0.5 ul |
| RNase Free Water | - | - | 4.5 µl |
| Total Volume of Reaction | | | 10 µl |

**Table 7. TaqMan real-time PCR program for gene expression analysis**

| | Step | Temperature | Time | Repetitions |
|---|---|---|---|---|
| Hold Stage | Uracil-N-glycosylase activation | 50 ℃ | 2min | 1x |
| | Initial denaturation | 95 ℃ | 10min | 1x |
| PCR Stage | Denaturation | 95 ℃ | 15s | 40x |
| | Annealing and elongation | 60 ℃ | 1min | |

**Table 8. Gene Expression assays used for TaqMan gene expression analysis**

| Assay ID | Species and Gene Symbol | Gene Name |
|---|---|---|
| Hs99999905_m1 | Human *GAPDH* | Glyceraldehyde-3-phosphate dehydrogenase |
| Hs00906229_g1 | Human *CRIP1* | Cysteine Rich Protein 1 |
| Hs00354836_m1 | Human *CASP1* | Caspase 1 |
| Hs01555410_m1 | Human *IL-1β* | Interleukin 1 beta |
| Hs00174114_m1 | Human *IL-2* | Interleukin 2 |
| Hs01038788_m1 | Human *IL*-18 | Interleukin 18 |
| Hs00765730_m1 | Human *NF-KB* | Nuclear Factor Kappa B Subunit |
| Hs00193878_m1 | Human *SH2B3* | SH2B Adaptor Protein 3 |
| Mm02619580_g1 | Mouse *Actb* | Actin Beta |
| Mm03024075_m1 | Mouse *Hprt* | Hypoxanthine Phosphoribosyltransferase |
| Mm01740671_mH | Mouse *Crip1* | Cysteine Rich Protein 1 |
| Mm00840904_m1 | Mouse *Nlrp3* | NLR Family Pyrin Domain Containing 3 |
| Mm00434228_m1 | Mouse *Il-1β* | Interleukin 1 beta |
| Mm00434256_m1 | Mouse *Il-2* | Interleukin 2 |
| Mm00446190_m1 | Mouse *Il-6* | Interleukin 6 |
| Mm00439616_m1 | Mouse *Il-10* | Interleukin 10 |
| Mm00434225_m1 | Mouse *Il-18* | Interleukin 18 |
| Mm00802529_m1 | Mouse *Adgre1* | Adhesion G Protein-Coupled Receptor E1 |
| Mm99999056_m1 | Mouse *Ccl2* | C-C motif chemokine ligand 2 |
| Mm01277161_m1 | Mouse *Cd44* | CD44 molecule |

| | | |
|---|---|---|
| Mm00516023_m1 | Mouse *Icam1* | Intercellular adhesion molecule 1 |
| Mm00434455_m1 | Mouse *Itgam* | Integrin subunit alpha M |

#### 2.2.4.4 Statistical analysis

The cDNAs threshold cycle (Ct) values, obtained by RT-qPCR, were analyzed through the comparative ΔΔCT method according to the following formula: ΔΔCt = ΔCt (sample) – ΔCt (control). ΔCt was calculated as follow: ΔCt = Ct (target gene) - Ct (housekeeping gene).

## 2.2.5 Immunoblot analysis

#### 2.2.5.1 Protein lysate preparation

Cells were lysed in RIPA buffer containing protease and phosphatase inhibitor cocktail on ice for 30 min and then centrifuged at 14000 rpm for 30 min at 4 ℃. After centrifugation, clear supernatant was transferred to new tubes and frozen at -80 ℃ until further BCA and immunoblot analysis.

#### 2.2.5.2 Bicinchoninic acid (BCA) assay

The BCA assay was conducted to measure the concentration of protein in samples. The mechanism of protein quantification using this method is based on the biuret reaction. When protein is placed in an alkaline system containing $Cu2^{+}$ a colored complex can form between the peptide bonds of the protein and the copper atoms (Smith et al. 1985). During biuret reaction, $Cu2^{+}$ is reduced to a cuprous ion $Cu^{+}$ which then can chelate with 2 molecules of bicinchoninic acid. As a result of this reaction, $Cu^{+}$ bicinchoninic acid complex is formed and its specific violet color shows absorbance at 562 nm and concentration of proteins can be quantified by comparing the absorbance of samples with a standard curve, made from purified bovine serum albumin.

BCA standard dilutions were prepared according to the manufacturer's instructions. Samples were diluted in a 1:5 or 1:10 ratio and as well as standard samples pipetted on the 96-well plate in duplicates for double determination. BCA reagent A from BCA Kit was mixed with BCA reagent B in the proportion of 50 parts of reagent A to 1 part of reagent B and 200 µL of this mixture was added to each well. The plate was slightly shacked and incubated at 37 ℃ for 30 min. Subsequently, the plate was cooled down to room temperature and absorbance was determined at 562 nm using Microplate reader Infinite 200/200Pro. The protein concentration of each sample was calculated according to the standard curve and the measured value.

#### 2.2.5.3 Sodium dodecyl sulfate-polyacrylamide gel electrophoresis

Sodium dodecyl sulfate-polyacrylamide gel electrophoresis (SDS–PAGE) is the mostly used electrophoresis technique for protein separation. It is based on the usage of polyacrylamide gel that creates a gel matrix with pores of different sizes. Proteins

migrate through the gel matrix at different rates according to their molecular masses. Proteins with lower molecular weight move more quickly through the gel than those with higher molecular weight. The polyacrylamide gel consists of two sections: stacking gel and separating gel. After applying the samples with denaturation buffer (Laemmli buffer), which gives proteins negative charge and reduces them to the primary structure, an electric field can be created in the system and proteins as charged molecules will migrate from the negatively charged top to the positively charged bottom dividing by their molecular masses in the separating gel.

Polyacrylamide gel with a concentration of 12% was prepared according to Table 9. APS and TEMED were added at the end step to initiate the polymerizing reaction. Firstly, separating gel was poured smoothly into the space between spacer and glass plate in the casting frame and allowed to polymerize for 20 min. Stacking gel solution was prepared and poured over the separating gel. A plastic comb was placed inside, and polyacrylamide gel construction was left to polymerize. The gels were stored at 4 ℃ covered in wet tissues.

Before electrophoresis, Protein samples were balanced to the desired concentration with RIPA buffer according to BCA assay results. 6x Loading buffer (Laemmli) were added to the samples to 1x final concentration, and denaturated at 95 ℃ for 10 min, then cooled to room temperature. Running gel apparatus was assembled and the tank was filled with SDS-running buffer, subsequently, samples were loaded, and the electrophoresis cell was connected to the power supply. The run proceeded at 100 V for about 30 min until the dye reached the level of separating gel and then on 120 V until it reached the gel's bottom.

**Table 9. Stacking and Separating gel preparation scheme**

| Reagents and chemicals | Stacking gel, 4% | Separating gel, 12% |
|---|---|---|
| 40% Acrylamide | 1 ml | 4.5 ml |
| 1 M Tris-HCl pH 8.8 | - | 5.625 ml |
| 0.5 M Tris-HCl pH 6.8 | 2.52 ml | - |
| $H_2O$ | 6.36 ml | 4.615 ml |
| 10% SDS | 100 µl | 150 µl |
| 10% APS | 50 µl | 100 µl |
| TEMED | 10 µl | 10 µl |
| Total | 10 ml | 15 ml |

#### 2.2.5.4 Protein transfer and antibody incubation

After SDS-PAGE the immunoblot was prepared. Proteins were transferred to membranes with Bio-Rad's Trans-Blot Turbo system. After completed transfer, the membrane was placed in the 50 ml tubes with 5% Blocking buffer and incubated on a shaker for 1h at room temperature. The membrane was washed 3 times with TBST

and incubated with a primary antibody diluted as described in the antibody list above (2.1.5). Subsequently, the membrane was washed 3 times with TBST and the secondary antibody was diluted at 1:10.000 in 1% BSA in TBST and incubated with the membrane for 1 h. Afterward, membrane was washed with TBST 3 times and stored at 4 ℃ or visualized directly.

#### 2.2.5.5 Protein detection and visualization

ECL Clarity™ or FEMTO SuperSignal™ was used according to the manufacturer's instructions. Chemiluminescence was acquired by Fusion SOLO S. Detection and densitometric evaluations were performed using the VisionCapt software. All data were edited and quantified using the VisionCapt program and statistical analysis was performed using GraphPad Prism 8.

### 2.2.6 Cell viability and cytotoxicity assay

THP1 single cell lines transfected with specific shRNA against CRIP1 (shCRIP1) or control shRNA (shCtrl) were characterized with cell viability and cytotoxicity assay. Cell viability was determined using the RealTime-Glo™ MT Cell Viability Assay kit (Promega) and cell cytotoxicity was determined using CellTox™ Green Cytotoxicity Assay kit (Promega).

In the Cell Viability Assay, a non-lytic NanoLuc Luciferase reaction occurs in the culture medium. NanoLuc Luciferase and MT Cell Viability Substrate are added to cell culture media. The MT Cell Viability Substrate is reduced to a NanoLuc substrate by metabolically active cells. The NanoLuc substrate diffuses from cells into the surrounding culture medium and is rapidly used by NanoLuc Enzyme to produce a luminescent signal. The signal correlates with the number of viable cells. Dead cells do not reduce the substrate and produce no signal.

The Cytotoxicity Assay measures changes in membrane integrity that occur as a result of cell death. The assay system uses a proprietary asymmetric cyanine dye that is excluded from viable cells but preferentially stains the dead cells' DNA. When the dye binds DNA in compromised cells, the dye's fluorescent properties are substantially enhanced. Viable cells produce no appreciable increases in fluorescence. Therefore, the fluorescent signal produced by the dye binding to the dead-cell DNA is proportional to cytotoxicity.

Cell viability and cytotoxicity assay were performed multiplexed following the manufacturer's protocol. Cells were counted and resuspended in growth medium containing 1x MT Cell Viability Substrate, 1x NanoLuc Enzyme and 1x CellTox™ Green Dye, then plated at 1000 cells/well in 100 µl total volume of medium in a 96-well opaque-walled tissue culture plate. Cells were then incubated at 37 ℃ in a $CO_2$ incubator for 72 h, luminescence and fluorescence signal were recorded every 6 hours. All data were plotted as a line graph.

### 2.2.7 Lumit™ human IL-1β immunoassay

The Lumit™ Human IL-1β Immunoassay is based on NanoLuc® Binary Technology (NanoBiT®). NanoBiT is a luminescent structural complementation system designed for biomolecular interaction studies. The system is composed of two subunits, Large BiT (LgBiT; 18kDa) and Small BiT (SmBiT; 11 amino acid peptide), that have been optimized for stability and minimal spontaneous association. In this assay, a sample is incubated with a pair of anti-human IL-1β monoclonal antibodies covalently labeled with SmBiT or LgBiT. When the labeled antibodies recognize and bind to released IL-1β, the complementary LgBiTs and SmBiTs are brought into proximity, thereby reconstituting NanoBiT® enzyme and generating luminescence in the presence of the Lumit™ substrate. Luminescence generated is directly proportional to the amount of analyte present in the sample.

In this experiment, shCRIP1 and shCtrl cells were primed with 1 μg/ml LPS for 3 hours for inflammasome formation with or without activation by 30 min incubation with 5 mM ATP. Subsequently, supernatant and cells were collected separately, and the cells were lysed with 50 μl digitonin (0.02%). Fluorogenic Live Cell Substrate (GF-AFC Substrate) was added to the cell medium during treatment to measure the relative number of viable cells.

For IL-1β immunoassay, a 2x Anti hIL-1β antibody mixture was prepared by diluting both antibodies (Anti-hIL-1β mAb-SmBiT and Anti-hIL-1β mAb-LgBiT) 1:500 into normal culture medium immediately before use. 50 μl/well of 2x Anti hIL-1β antibody mixture was then dispensed to 50 μl/well of standards, supernatant or cell lysates in a new 96-well opaque-walled tissue culture plate, and briefly mixed with a plate shaker. The plate was incubated at 37℃ in a $CO_2$ incubator for 90 min. Subsequently, 5x Lumit™ Detection Reagent was prepared by diluting a 20x Lumit™ Detection Substrate into Lumit™ Detection Buffer. After incubation, the assay plate was equilibrated to room temperature for 10 min, then dispensed with 25 μl Lumit™ Detection Reagent per well and mixed briefly. Luminescence was read after 5 min incubation. The concentration of human IL-1β was calibrated from a dose-response curve based on the reference standards.

Data were expressed as mean±SEM and were relative to the corresponding cell viability. Statistical analysis was performed using Two-way ANOVA followed by Tukey's multiple comparison test. Differences were considered significant when P-value < 0.05.

### 2.2.8 Human IL-18 ELISA assay

The supernatant samples from Lumit™ IL-1β Human Immunoassay experiments were also used to measure IL-18 levels. IL-18 expression was detected via the Human IL-18 ELISA Assay (MBL International Corporation). The Human IL-18 ELISA Kit

measures human IL-18 by ELISA. This assay uses two monoclonal antibodies against two different epitopes of human IL-18.

A total value of 100 µl diluted supernatant samples and standards were incubated in the microwells coated with anti-human IL-18 monoclonal antibody for 60 min at room temperature. After washing 4 times with wash solution, 100 µl peroxidase conjugated anti-human IL-18 monoclonal antibody was added into the microwells and incubated for 60 min at room temperature. After 4 times washing, 100 µl substrate reagent mixed with the chromogen was allowed to incubate in dark for an additional 30 min at room temperature. Then, 100 µl of stop solution was added to each microwell to terminate the enzyme reaction and to stabilize the color development. The optical density (O.D.) of each microwell was measured at 450 nm. The concentration of human IL-18 was calibrated from a dose-response curve based on the reference standards.

Data were expressed as mean±SEM and were relative to the corresponding cell viability. Statistical analysis was performed using Two-way ANOVA followed by Tukey's multiple comparison test. Differences were considered significant when P-value < 0.05.

### 2.2.9 Murine models of inflammation

Animal models are indispensable in cardiac and inflammation research. The collaboration with the Institute of Immunology UKE, Prof. Hans-Willi Mittrücker allowed us to analyze the expression of *Crip1* and the cytokine dysfunction of murine models for inflammation and kidney disease which were already published (Krebs et al. 2020) to verify the results observed in *in vitro* part of this thesis.

The murine infection model was established by intravenous infection with Staphylococcus aureus (*S.aureus*). Intravenous infection of mice with *S. aureus* induced the highest bacterial titers transiently in the kidney than in other tissues. Mice were treated with ampicillin for 7 days to curb chronic infection 14 days after *S.aureus* infection and were completely recovered from infection at day 30. Bacteria were cleared and mice showed normal renal function and morphology. Kidney RNA samples at day 3, 10, and 30 post-infection were kindly provided by Prof. Mittrücker's working group to analyze *Crip1* and pro-inflammatory cytokines expression in this thesis.

An established experimental crescentic glomerulonephritis (cGN) model (nephrotoxic nephritis model) was also provided by Prof. Hans-Willi Mittrücker's working group (Krebs et al. 2020, Kurts et al. 2013). Anti-GBM sheep Igs bind within the glomerulus after passive transfer and provoke a T cell response against the deposited antigen. This response results in the formation of glomerular crescents, tubulointerstitial damage, and loss of renal function resembling multiple aspects of human cGN. 10 days after sheep Ig application, kidney samples were analyzed. We were provided with RNA samples from these mice and analyzed in this thesis as another murine inflammation

model.

### 2.2.10 Statistical analysis

Immunoblot data were quantified using the VisionCapt program, and calculations were edited using Excel software. GraphPad Prism 8 was used for graphing and statistical analysis. Data were expressed as mean ±SEM.

Data between the two groups were analyzed and compared using Student's t-test for normal distribution, otherwise Mann-Whitney test. Two-way ANOVA followed by Tukey's multiple comparison test was used when the two groups being compared had additional treatment conditions. Two-way ANOVA followed by Sidak's multiple comparison test was used in the cell viability and cytotoxicity assay. The Mann-Whitney test was used for comparison between the three groups. P-values less than 0.05 were considered statistically significant.

# 3. Results

To elucidate the role of CRIP1 on inflammation and CVDs, a CRIP1-downregulated cell model via shRNA was established in the monocytic-like cell line THP-1 using an *in vitro* approach. Subsequently, cell cytotoxicity and viability were monitored, and the alterations in cytokines and chemokines known to be involved in CVDs were detected after induction of inflammation by LPS and ATP. In an *ex vivo* approach, *Crip1* mRNA expression and its correlations with mRNA expression levels of inflammatory mediators were investigated in established mouse inflammation and kidney disease models.

## 3.1 Establishment of CRIP1-downregulated cell model

### 3.1.1 Downregulation of CRIP1 in THP-1 cells by shRNA

It is known from transcriptome analysis of human populations, that CRIP1 expression in human monocytes is associated with blood pressure. Therefore, the monocytic-like cell line THP-1 was chosen as *in vitro* model to investigate alterations in CRIP1 and inflammatory mediators expression upon CRIP1 knockdown and stimulation with pro-inflammatory reagents.

In THP-1 cells, stably CRIP1 downregulation was generated using a specific shRNA against CRIP1 (shCRIP1). THP-1 cells were transfected with shRNA plasmid control (shCtrl) or against CRIP1 by lipofectamine-based method. After selection by adding puromycin, cells were sorted into single clones and expanded to single-clone populations.

In total 16 single-clone populations transfected with shCRIP1 were generated. Cells from each single-clone population were harvested. RNAs were isolated and *CRIP1* expression was detected at the mRNA level by real-time quantitative PCR. Protein lysates were generated from each single-clone population and CRIP1 protein expression was investigated using the immunoblotting technique. Glyceraldehyde 3-phosphate dehydrogenase (GAPDH) served as a loading control for CRIP1 protein normalization.

Figure 3 showed different CRIP1 expressions in THP-1 single-clone populations transfected with shCRIP1 plasmid. Reduced expression of CRIP1 was observed in all 16 shCRIP1 single-cell clones. In each clone, CRIP1 expression level was consistent at the transcriptional and translational levels. Clone 7 showed the most significant CRIP1 knockdown level, 82% at the mRNA level and 94% at the protein level, and was considered to the enough. Clone 7 was termed as “shCRIP1” for further investigation.

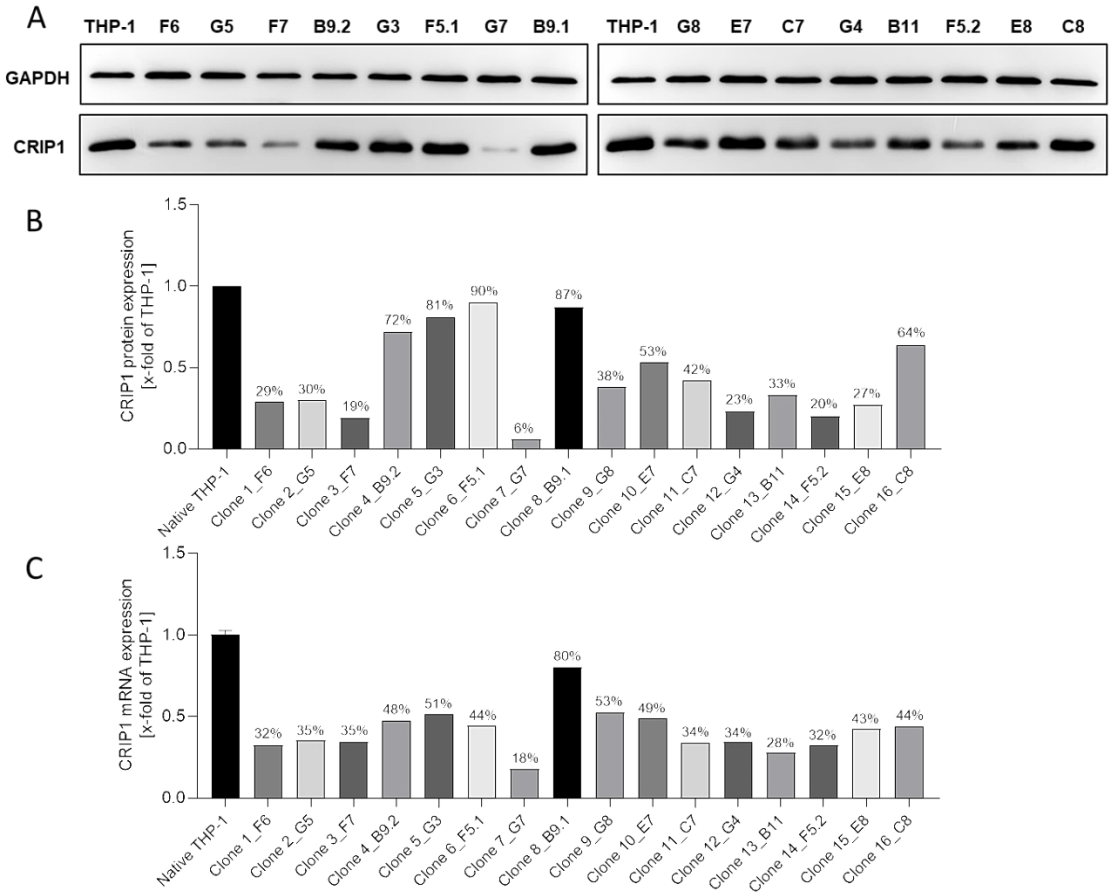


**Figure 3. Immunoblot and gene expression analysis of CRIP1-downregulated cells.** (**A and B**) Typical immunoblot and quantitative evaluation of CRIP1 protein expression normalized to GAPDH. **(C)** *CRIP1* mRNA expression normalized to *GAPDH* using ΔΔCt-method. Data are expressed as mean ±SEM relative to native THP-1. n= 1-2 biological replicates per group. The number above the columns showed the ratio of CRIP1 expression level to the control (native THP-1) in each group.

The downregulation of CRIP1 in shCRIP1 single-clone population remained stable after several cell passages. Figure 4 showed CRIP1 expression in THP-1 single-clone populations shCRIP1 and shCtrl. At both the transcriptional and translational levels, CRIP1 expression showed stably more than 80% reduction.

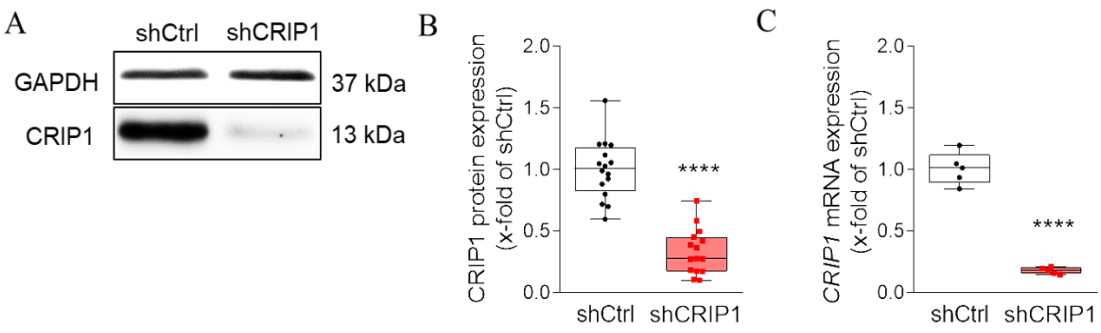


**Figure 4. Immunoblot and gene expression analysis of CRIP1-downregulated cells (shCRIP1) and control cell line (shCtrl).** (**A and B**) typical immunoblot and quantitative evaluation of CRIP1 protein expression normalized to GAPDH. (**C**) *CRIP1* mRNA expression normalized to *GAPDH* using ΔΔCt-method. Data are expressed as mean ±SEM relative to shCtrl. n= 5-16 biological replicates per group, Student's t-test. ****p<0.0001 vs. shCtrl.

## 3.1.2 Characterization of shCRIP1 and shCtrl cells

### 3.1.2.1 Morphology

After being transfected with shRNA plasmid, neither shCtrl nor shCRIP1 cells showed distinct morphological changes under microscopy compared with native THP-1 cells. All cells appeared as round-like, uniformly sized suspension cells as shown in Figure 5.

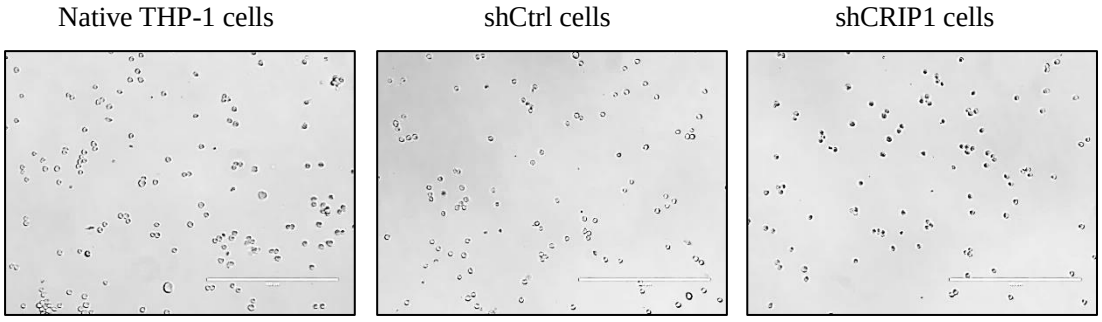


**Figure 5. Morphological representation of shCtrl and shCRIP1 cells.** The cells cultured in 6-well tissue plates were placed under a light microscope for observation and images were recorded under a 20x objective.

### 3.1.2.2 Cell viability and cytotoxicity

shCtrl and shCRIP1 cells exhibited similar cell viability profiles over a 72 hour monitoring period. Significant differences in cytotoxicity were observed from the

36-hour time point of monitoring, with shCRIP1 cells showing fewer cytotoxicity levels after longer periods in culture (Figure 6).

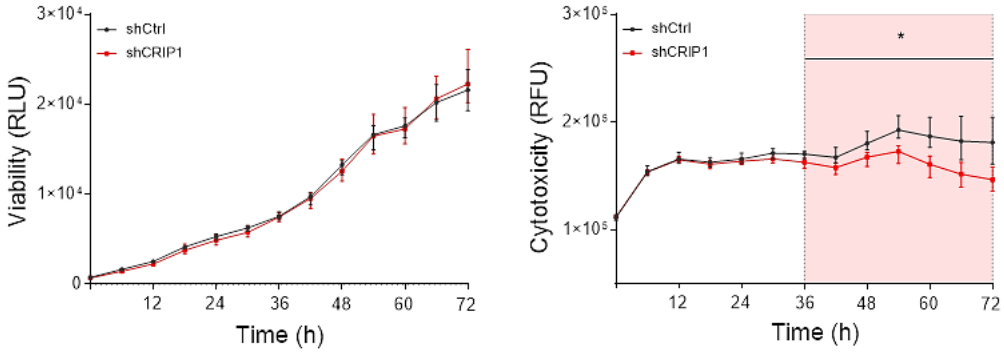


**Figure 6. Cell viability and cytotoxicity of shCtrl and shCRIP1 cells.** Cells were seeded in 96-well plate each, viability (luminescence, RLU) and cytotoxicity (fluorescence, RFU) were determined in the same well every 6 h for 72 h. Data are expressed as mean±SEM. n= 7 biological replicates per group, Two-way ANOVA followed by Sidak's multiple comparison test. *p<0.05 vs. shCtrl.

## 3.2 Role of CRIP1 in regulating inflammation pathway in THP-1 cells

### 3.2.1 CRIP1 and cytokines expression after inflammation

A well-described *in vitro* THP-1 cell model of inflammation (Grahames et al. 1999, Chanput et al. 2010) was established using LPS to explore the inflammatory regulation effects of CRIP1. ShCRIP1 cells were stimulated with LPS at the concentration of 1 µg/ml. After 3 hours cells were harvested and RNA was isolated. Subsequently, gene expression of *IL-1β, IL-18, CASP-1, NF-κB, CCL2* and *SH2B3* was investigated using qPCR analysis. Cell stimulation was performed in duplicates to provide reproducibility (Figure 7).

In THP-1 cells, downregulation of CRIP1 via shRNA significantly altered the mRNA expression of cytokines known to be involved in Hypertension and CVDs (*IL-1β, IL-18, CASP-1, NF-κB, CCL2*, and *SH2B3*) after induction of inflammation by LPS.

Downregulation of CRIP1 did not affect the basal gene expression of *IL-1β*, *NF-κB* and *CCL2*, while basal gene expression of *IL-18*, *CASP-1* and *SH2B3* was reduced in shCRIP1 cells, compared with shCtrl cells. In shCtrl cells, *IL-1β, CASP-1, NF-κB* and *CCL2* mRNA expression was significantly increased after LPS stimulation, an elevated trend was also observed in the expression of *IL-18* and *SH2B3*. Compared to shCtrl cells, *IL-1β* ($p<0.001$), *IL-18* ($p<0.01$), *CASP-1* ($p<0.0001$), *NF-κB* ($p<0.0001$),

*CCL2* ($p<0.001$), and *SH2B3* ($p<0.05$) expression in shCRIP1 cells were all significantly reduced after LPS treatment.

All the elevated genes expression in response to inflammation was diminished in CRIP1-downregulated cells, of which the most significant gene was *IL-1β*. After LPS treatment, *IL-1β* expression showed a ~100-fold increase in shCtrl cells, while only mildly elevation was observed in shCRIP1 cells.

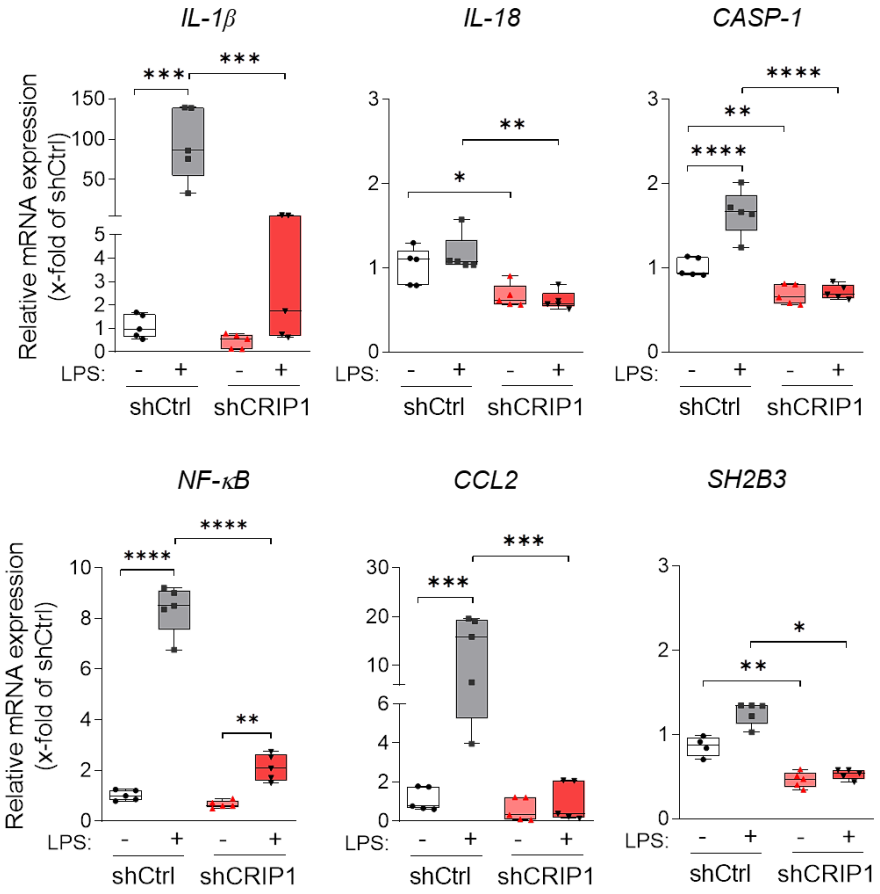


**Figure 7. Gene expression analysis of inflammatory mediators known to contribute to the pathogenesis of CVDs.** Cells were treated with lipopolysaccharide (LPS, 1 µg/ml) for 3 hours before harvest. *IL-1β, IL-18, CASP-1, NF-κB, CCL2,* and *SH2B3* mRNA expression were normalized to *GAPDH* using ΔΔCt-method. Data are expressed as mean ±SEM relative to shCtrl untreated "-". n= 5 biological replicates per condition, Two-way ANOVA followed by Tukey's multiple comparison test. *p<0.05; **p<0.01; ***p<0.001; ****p<0.0001.

### 3.2.2 IL-1β protein expression and IL-1β release after NLRP3 inflammasome activation

In shCtrl cells, *IL-1β*, *IL-18*, *CASP-1* and *NF-κB* mRNA expression was significantly increased or showed elevated trend after LPS stimulation. The most significant gene IL-1β showed a nearly 100-fold increase in expression. However, all the elevated genes expression in response to inflammation was diminished in shCRIP1 cells. After CRIP1 downregulation by shRNA, LPS stimulation only mildly increased the mRNA expression of these cytokines in cells. Interestingly, these cytokines are all key components of the NLRP3 inflammasome signaling pathway. IL-1β and IL-18 secretions are results and important markers of NLRP3 inflammasome activation (Van de Veerdonk et al. 2011). Thus IL-1β protein expression and release were then investigated to further confirm whether CRIP1 is involved in the activation of NLRP3 inflammasome in THP-1 cells.

THP-1 cells have the potential to be differentiated into macrophage-like cells. They were found to be more sensitive to pro-inflammatory inducers after differentiation than monocytes and showed higher expression of inflammatory cytokines (Chanput et al. 2010). In this experiment, shCtrl and shCRIP1 cells were investigated as both monocytes and macrophages to see how they behave under treatment conditions.

Cells were primed with 1 μg/ml LPS for 3 hours for inflammasome formation with additional activation by 30 min incubation with 5 mM ATP. Fluorogenic Live Cell Substrate (GF-AFC Substrate) was added to the cell medium during treatment to measure cell viability and data were normalized correspondingly. In terms of cell viability, there was no significant difference between shCtrl cells and shCRIP1 cells as both monocytes and macrophages (Figure 8).

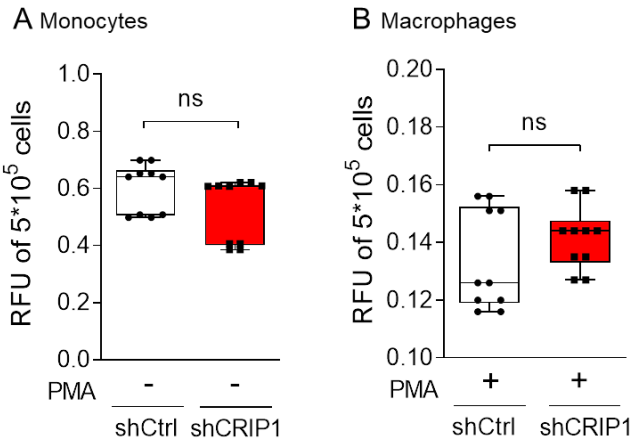


**Figure 8. Cell viability assay of the THP-1 monocytes and macrophages.** shCtrl and shCRIP1 cells were differentiated with PMA or undifferentiated. Fluorogenic Live Cell Substrate (GF-AFC Substrate) was added to the cell medium during treatment. Subsequently,

the viability of the cells was assessed by detecting fluorescence according to the manufacturer's recommendations. Relative fluorescence units (RFU) were then calculated from each sample. Data are expressed as mean ±SEM relative to shCtrl. n= 5 biological replicates per group, Student's t-test.

The IL-1β protein expression and release measurement showed that, as monocytes (Figure 9, A-B), shCtrl cells showed a lower IL-1β basal concentration level than shCRIP1 cells ($p<0.05$). Following LPS/ATP treatment, IL-1β release from both shCtrl and shCRIP1 cells was significantly higher but no significant difference between the two groups was observed (Figure 9A). IL-1β expression was similar in shCtrl and shCRIP1 cells before treatment. The addition of LPS significantly increased IL-1β protein expression in shCtrl cells but not in shCRIP1 cells (Figure 9B, $p<0.01$), consistent with the effect on mRNA expression. Lower IL-1β protein expression was also observed in shCRIP1 cells after NLRP3 inflammasome activation (Figure 9B, $p<0.0001$).

48h PMA treatment significantly increased the IL-1β expression in THP1 cells. As differentiated macrophages (Figure 9, C-D), shCtrl and shCRIP1 cells showed the same IL-1β basal release, nevertheless less IL-1β was released from shCRIP1 cells to the supernatant after NLRP3 activation (Figure 9C, $p<0.0001$). Consistently, IL-1β expression was lower in shCRIP1 cells compared with shCtrl cells, also lower after NLRP3 inflammasome formation and activation (Figure 9D, $p<0.0001$). CRIP1 downregulation avoids the activation of the NLRP3 inflammasome by decreased IL-1β protein content and secretion.

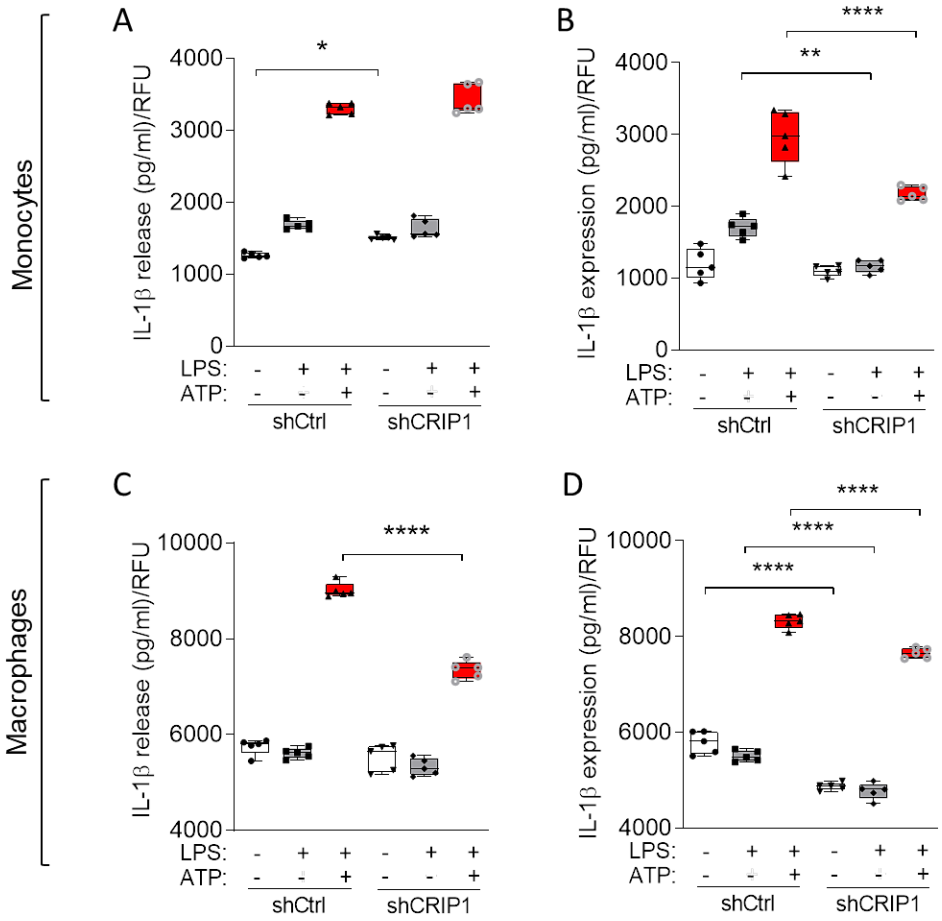


**Figure 9. IL-1β release and IL-1β protein expression after activation of the inflammasome via LPS/ATP.** (**A and B**) THP-1 monocytes were treated with medium containing LPS (1 µg/ml) for 3 hours followed by activation of the inflammasome (ATP, 5 mM) for 30 min. IL-1β release was measured in the supernatant. For IL-1β protein expression, the cells were lysed with digitonin (0.02%). IL-1β was determined using a commercial luminescence kit according to manufacturer instructions. (**C and D**) Cells were differentiated with Phorbol 12-Myristate 13-Acetate (PMA, 50 ng/ml) for 48 hours. The culture medium was removed, replaced with medium containing LPS (1 µg/ml), and incubated for 3 hours followed by activation of the inflammasome (ATP, 5 mM) for 30 min. IL-1β release and IL-1β protein expression were determined using the same approach as monocytes. Data are expressed as mean±SEM and are relative to the corresponding cell viability. n= 5 biological replicates per condition, Two-way ANOVA followed by Tukey's multiple comparison test. ****p<0.0001.

### 3.2.3 IL-18 protein release after NLRP3 inflammasome activation

Based on the results that IL-1β protein expression and secretion were regulated by CRIP1 knockdown in THP-1 cells during NLRP3 inflammasome activation, another important marker for NLRP3 inflammasome activation IL-18 was also investigated to

further confirm that the activation of the NLRP3 inflammasome in THP-1 cells can be diminished by CRIP1 downregulation.

In shCtrl and shCRIP1 monocytes (Figure 10A), IL-18 showed the same basal release, and it was significantly increased after LPS and ATP stimulation. Interestingly, after LPS induced NLRP3 formation, shCRIP1 cells released more IL-18, after activation of the NLRP3 inflammasome via ATP, the releasement was particularly lower in shCRIP1 cells compared to shCtrl cells ($p<0.0001$). IL-18 release was almost undetectable after cells were differentiated into macrophages with PMA (Figure 10B).

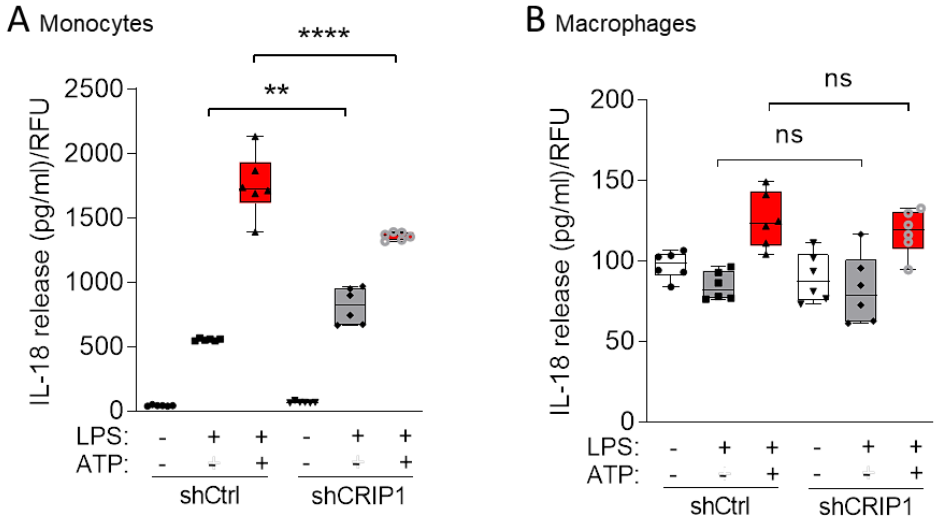


**Figure 10. IL-18 release after formation and activation of the inflammasome via LPS/ATP.** (**A**) THP-1 monocytes were treated with medium containing LPS (1 µg/ml) for 3 hours followed by activation of the inflammasome (ATP, 5 mM) for 30 min. IL-18 release in the supernatant was determined using a commercial Elisa kit according to manufacturer instructions. Cell viability was measured by adding Fluorogenic Live Cell Substrate (GF-AFC Substrate) to the medium during treatment. (**B**) Cells were differentiated with Phorbol 12-Myristate 13-Acetate (PMA, 50 ng/ml) for 48 hours. The culture medium was removed, replaced with medium containing LPS (1 µg/ml), and incubated for 3 hours followed by activation of the inflammasome (ATP, 5 mM) for 30 min. IL-18 release was determined using the same approach as monocytes. Data are expressed as mean ±SEM and are relative to the corresponding cell viability. n= 5 biological replicates per condition, Two-way ANOVA followed by Tukey's multiple comparison test. ****$p<0.0001$.

## 3.3 Induction of CRIP1 and target cytokines in murine inflammation models

In collaboration with the Institute for Immunology, University Medical Center Hamburg-Eppendorf (Prof. Hans-Willi Mittrücker), we analyzed the expression of

*Crip1* and inflammatory mediators in established murine models for inflammation (Krebs et al. 2020) to verify the results observed in the *in vitro* part of this thesis.

### 3.3.1 Analysis of CRIP1 and inflammatory markers expression in mouse infection model

The mouse infection model was established by intravenous infection with *S.aureus*. Mice were completely recovered from infection at day 30 (Krebs et al. 2020). Intravenous infection of mice with *S. aureus* induced the highest bacterial titers transiently in the kidney than in other tissues.

Analysis of renal mRNA revealed that *Crip1* expression was upregulated at day 10 post-infection ($P<0.05$). At day 30 post-infection, mice were cleared of the bacteria by the immune answer, or by anti-infective treatment with oral ampicillin. *Crip1* expression decreased to baseline levels in mice recovered from infection at day 30. There was no significant difference in *Crip1* expression between control mice, mice that healed spontaneously after infection, and mice that were cured by oral ampicillin (Figure 11). *Nlrp3* mRNA expression was increased in *S.aureus* infected mice on day 3, and 10 post-infection ($P<0.001$), and remained elevated after the clearance of *S.aureus* ($P<0.01$). In mice treated with oral ampicillin after infection, *Nlrp3* expression level returned to the same level as control mice at day 30 post-infection (Figure 12).

Inflammatory cytokines *Il-1β*, *Il*-2, *Il-6*, *Il-10*, and *Il-18* mRNA expression were also detected in kidney samples at day 3, 10, and 30 post-infection. The correlations between cytokines and *Crip1* expression were analyzed (Figure 13). At day 10 post-infection, increased levels of *Crip1* expression were positively correlated with the high mRNA expression levels of pro-inflammatory cytokines.

Additionally, markers known for leukocyte infiltration (*Adgre1*, *Ccl2*, *Cd44*, *Icam1* and *Itgam*) mRNA expression at day 3, 10, and 30 post-infection were detected (Figure 14). *Adgre1*, *Ccl2*, *Cd44*, *Icam1* and *Itgam* expression increased significantly from day 3 and then gradually decreased as the infection recovered, showing a consistent regulation trend with *Crip1*.

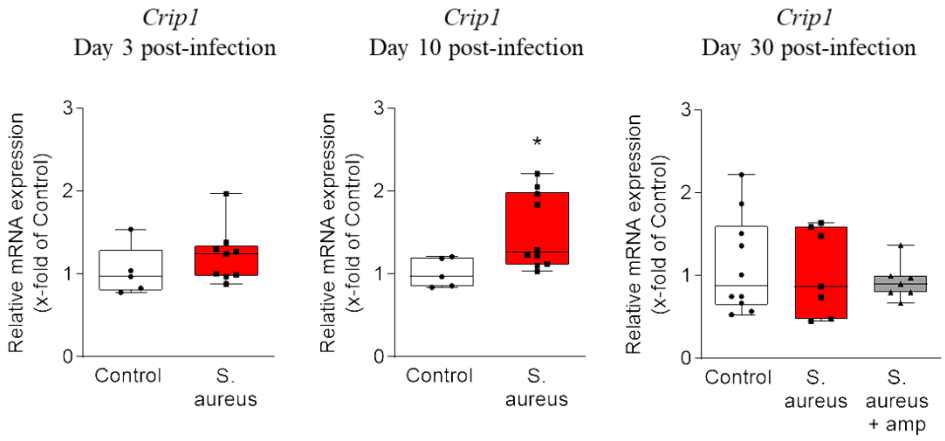


**Figure 11. *Crip1* mRNA expression at day 3, 10, and 30 post-infection.** Mice were intravenously infected with *S. aureus* and then treated with ampicillin for 7 days to curb chronic infection 14 days after *S. aureus* infection. Kidney samples at day 3, 10, and 30 post-infection were used to analyze *Crip1* expression by qPCR. mRNA expression was accessed by ΔΔCt-method normalizing *Crip1* Ct-values to the geometrical mean of *Actb/Hprt*. *p<0.05 vs. Control; Mann-Withney test.

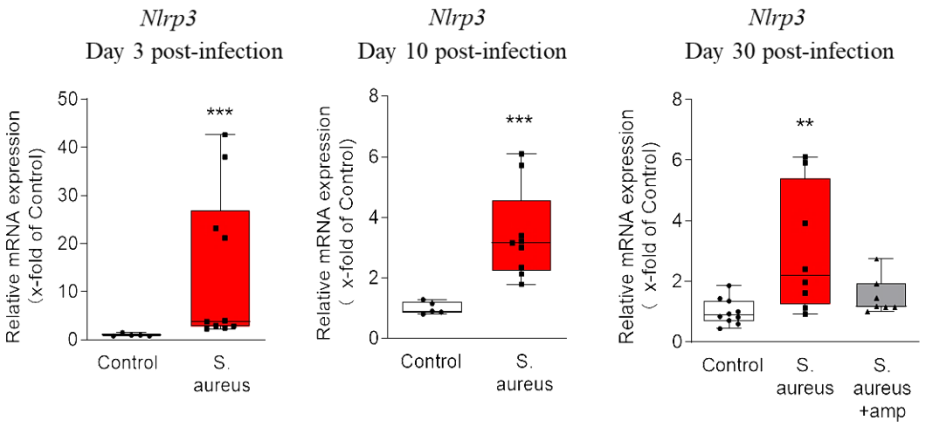


**Figure 12. *Nlrp3* mRNA expression at day 3, 10, and 30 post-infection.** Mice were intravenously infected with *S.aureus* and then treated with ampicillin for 7 days to curb chronic infection 14 days after *S.aureus* infection. Kidney samples at day 3, 10, and 30 post-infection were used to analyze *Nlrp3* expression by qPCR. mRNA expression was accessed by ΔΔCt-method normalizing *Nlrp3* Ct-values to the geometrical mean of *Actb/Hprt*. **p<0.01; ***p<0.001 vs. Control; Mann-Withney test.

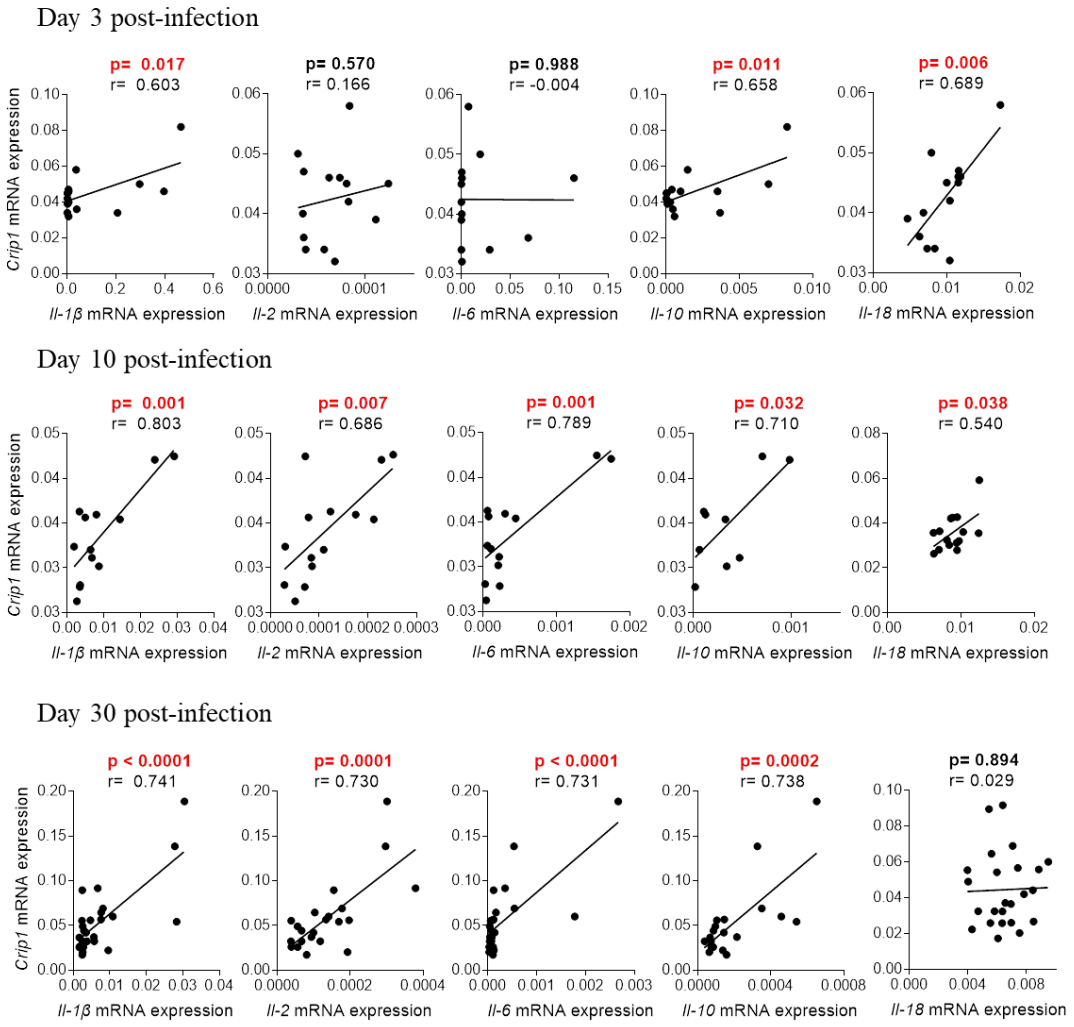


**Figure 13. Analysis of inflammatory cytokines correlating with *Crip1*.** *Il-1β*, *Il-2*, *Il-6*, *Il-10*, *Il-18*, and *Crip1* mRNA expression were detected in kidney samples at day 3, 10, and 30 post-infection. Significant positive correlations between *Crip1* and inflammatory mediators are shown in red. Scatterplots demonstrated the correlation between Ct-values of *Crip1* and inflammatory cytokines.

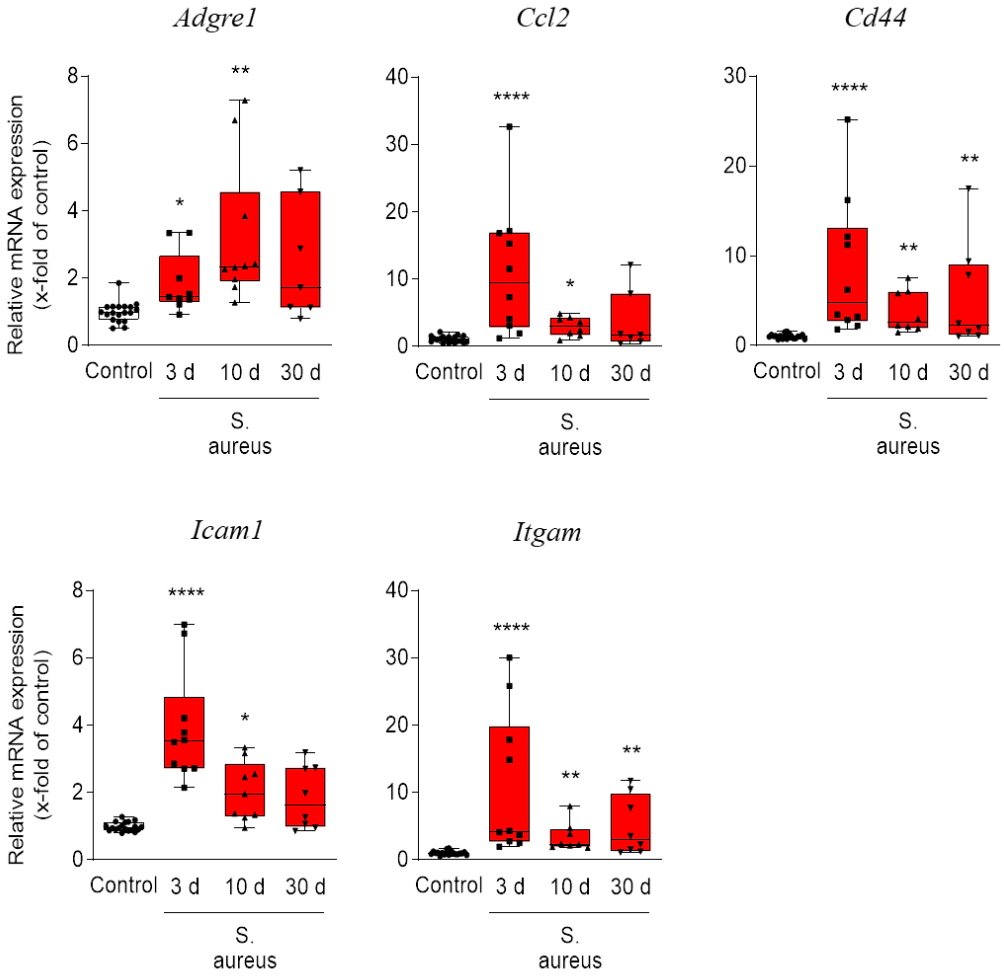


**Figure 14. Analysis of leukocyte infiltration markers.** *Adgre1*, *Ccl2*, *Cd44*, *Icam1* and *Itgam* mRNA expression were detected in kidney samples at day 3, 10, and 30 post-infection. mRNA expression was accessed by ΔΔCt-method normalizing Ct-values to the geometrical mean of *Actb/Hprt*. *p<0.05; **p<0.01; ****p<0.0001 vs. Control; Mann-Withney test.

### 3.3.2 Analysis of CRIP1 and inflammatory markers expression in mouse nephrotoxic nephritis (NTN) model

An established experimental crescentic glomerulonephritis (cGN) model (a nephrotoxic nephritis model) (Krebs et al. 2020, Kurts et al. 2013) was used. We were provided by Prof. Hans-Willi Mittrücker's working group with mRNA samples from these mice and analyzed in this thesis as another murine inflammation model.

Anti-GBM sheep Igs bind within the glomerulus after passive transfer and provoke a T cell response against the deposited antigen. This response results in the formation of glomerular crescents, tubulointerstitial damage, and loss of renal function resembling multiple aspects of human cGN. 10 days after sheep Ig application, kidney samples

were analyzed. *Crip1* and pro-inflammatory cytokines expression were determined using the gene expression analysis methods (Figure 15).

Upon induction of experimental glomerulonephritis, *Nlrp3*, *Il-1β*, *Il-2*, *Il-6*, *Il-10*, and *Il-18* mRNA expression was increased in the renal cortex. *Crip1* mRNA expression was also increased and correlated to the elevated cytokines and *Nlrp3* expression, underlying CRIP1's participation in inflammasome activation.

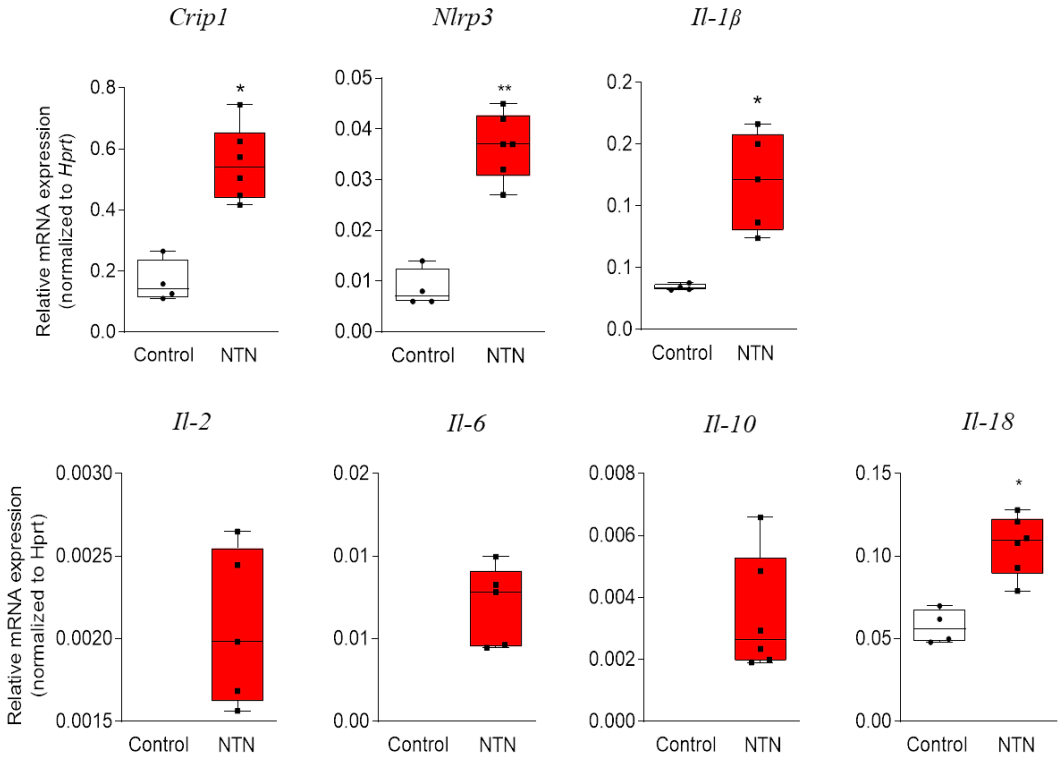


**Figure 15. mRNA expression of *Crip1* and inflammatory markers in NTN model of crescentic glomerulonephritis (cGN).** An established murine experimental cGN model was induced, and kidneys were analyzed 10 days later. *Crip1*, *Nlrp3*, *Il-1β*, *Il-2*, *Il-6*, *Il-10*, and *Il-18* mRNA expression were normalized to *Hprt* using ΔCt-method. Data are expressed as mean ±SEM. *p<0.05; **p<0.01 vs. Control; Student's t-test.

# 4. Discussion

Hypertension is a major global health challenge. It affects ~30% of adults and is a leading risk factor for major cardiovascular events, chronic kidney disease, heart failure, cognitive impairment and dementia (Iadecola et al. 2016, Whelton et al. 2018). An increasing number of researches point to the importance of inflammation and immunity in hypertension and CVD. The role of the inflammasome and its key cytokines IL-1β and IL-18 in the development of hypertension has also been highlighted (Pasqua et al. 2018, Norlander et al. 2018).

CRIP1 is a member of the LIM protein family. Recent studies have revealed that CRIP1 is closely related to the development of various cancers and CVDs, thus greatly enhancing the value of CRIP1. In a population-based transcriptomic study of human monocytes, CRIP1 was identified to be strongly associated with blood pressure (Zeller et al. 2017). CRIP1 is highly expressed in immune cells and CRIP1 mRNA expression in monocytes associates with BP and is up-regulated by pro-hypertensive (AngII) modulation suggesting a link between CRIP1 and BP regulation through the immune system (Schweigert et al. 2021). So far, current studies of CRIP1 are not sufficient to explain the molecular mechanisms associated with the pathophysiology of hypertension.

This thesis work especially focused on the influence of CRIP1 on the regulation of the immune system and inflammation signaling pathway *in vitro* and *in vivo* models considering target genes involved in hypertension.

Major findings of this thesis were

i) CRIP1 regulated NLRP3 inflammasome pathway in monocytes by altering the key cytokines expression and secretion.

ii) CRIP1 influenced pyroptosis in monocytes.

iii) CRIP1 altered other genes and inflammatory cytokines known to be involved in CVDs in monocytes.

iv) CRIP1 associated with inflammatory pathways in the murine infection model.

v) CRIP1 associated with inflammatory pathways in the murine kidney disease model.

## 4.1 CRIP1 participated in the regulation of inflammatory pathways in monocytes

Recent attention has been focused on exploring the pathways and inflammatory mediators that immune cells use to drive high blood pressure and end-organ damage.

When immune cells become activated and/or are recruited to a target organ, they produce cytokines that determine the local inflammatory response, disrupting the regulation of blood pressure in these organs, and leading to hypertension. Many inflammatory cytokines have been studied to be involved in hypertension.

### 4.1.1 CRIP1 regulated NLRP3 inflammasome pathway in monocytes

To investigate the role of CRIP1 on inflammation in monocytes, we established a CRIP1-downregulated cell model via shRNA in a monocytic-like cell line THP-1. The results of this thesis showed that compared with the control cells, CRIP1expression reduced by ~80% in CRIP1-downregulated cells. CRIP1-downregulated cells and control cells showed no morphological differences by light microscopy.

To induce pro-inflammatory conditions, both cell lines were stimulated with LPS, cytokine gene expression known to be involved in CVDs were detected after induction of inflammation. Our results showed that in shCtrl cells, *IL-1β, IL-18, CASP-1* and *NF-κB* mRNA expression was significantly increased or showed elevated trend after LPS stimulation. This is consistent with the results previously observed in animal experiments (Hallquist et al. 1996). The most significant gene IL-1β showed a nearly 100-fold increase in expression. However, all the elevated genes expression in response to inflammation was diminished in shCRIP1 cells. After CRIP1 downregulation by shRNA, LPS stimulation only mildly increased the mRNA expression of these cytokines in cells. Interestingly, these cytokines are all key components of the NLRP3 inflammasome signaling pathway.

The NLRP3 inflammasome is a key multiprotein signaling complex, which is composed of NLRP3, an adaptor protein apoptosis-associated speck-like protein (ASC), and caspase-1 (Li 2015). The NLRP3 inflammasome in immune cells such as monocytes and macrophages may be activated by PAMPs, DAMPs or environmental stimuli (Schroder and Tschopp 2010).

NLRP3 inflammasome has a large number of chemically and structurally distinct activating signals, many of which are relevant to the pathogenesis of hypertension. For example, microcrystals of sodium urate, calcium oxalate and cholesterol are all powerful activators of NLRP3 inflammasomes, which might explain the well-established associations between hypertension and hyperuricemia, urolithiasis and atherosclerosis, respectively (Mazzali et al. 2001, Krishnan et al. 2014). A high extracellular salt concentration, such as might occur in the urine and renal tubulointerstitial space in individuals with hypertension, is also powerful priming and activating stimulus for NLRP3 in macrophages and epithelial cells (Prager et al. 2016). Finally, extracellular ATP, acting through P2X7 receptors, is a stimulus for NLRP3 activation, although there is limited information on extracellular ATP levels in hypertension (Palygin et al. 2013).

The activation of NLRP3 inflammasome is a two-step process including priming and triggering (Elliott and Sutterwala 2015). The priming is a process in which PAMPs, DAMPs or environmental stress are recognized by TLRs leading to the activation of the NF-κB pathway, which results in the upregulation of NLRP3 protein, pro-Casp-1, pro-IL-1β and pro-IL-18 level (Sutterwala et al. 2006). The triggering is a subsequent stimulus that activates the NLRP3 inflammasome by promoting the oligomerization of inactive NLRP3, ASC and pro-Casp-1, resulting in proteolytic cleavage of Casp-1 and the maturation of pro-inflammatory cytokines, IL-1β and IL-18, and induces pyroptosis (Frangogiannis 2014). IL-1β and IL-18 activated by Casp-1 are then released and trigger the activation of other immune cells, such as neutrophils, at the site of infection or tissue damage, thereby promoting an inflammatory response (Latz et al. 2013).

Current evidence suggests an important role for the NLRP3 inflammasome in the pathophysiological processes in hypertensive animal models. Expression of the various components of NLRP3 inflammasome (i.e. TLR4, NLRP3, ASC, Casp-1, IL-1β and IL-18) is increased in key blood pressure-regulating organs during hypertension, including the kidneys (Krishnan et al. 2016, Zhu et al. 2016, Fanelli et al. 2017), arteries (Sun et al. 2017, Ren et al. 2017, Ling et al. 2018), heart (Gan et al. 2018), and brains (Qi et al. 2016a, Avolio et al. 2018). Systemic reduction in inflammasome activity owing to a genetic deficiency of NLRP3, ASC or Casp-1 protects mice from developing hypertension and end-organ damage (Krishnan et al. 2016, Gong et al. 2016, Krishnan et al. 2019).

Similarly, targeted inhibition of inflammasome activity in specific tissues can have antihypertensive effects. For example, selective inhibition of NLRP3 expression or the inflammasome-derived cytokine IL-1β in the paraventricular nucleus reduced high-salt diet-induced hypertension and brain markers of oxidative stress and inflammation in rats (Qi et al. 2016b, Qi et al. 2016a). Transplantation of anti-inflammatory mesenchymal stem cells or infusion of a Casp-1 inhibitor into the renal medulla of Dahl salt-sensitive rats prevented salt-induced hypertension (Zhu et al. 2016). Similarly, suppression or deficiency of TLR4 ameliorates or prevents hypertension (Bomfim et al. 2012, Dange et al. 2015). Inactivation or deficiency of the P2x7 receptor ameliorates hypertension in the Dahl salt-sensitive rat (Ji et al. 2012). Suppression of NF-κB activation prevents hypertension in spontaneously hypertensive rats (Rodr ́guez-Iturbe et al. 2005). Deficiency of ASC ameliorates DOCA-salt hypertension (Krishnan et al. 2016).

In humans, circulating levels of IL-1β and IL-18 are elevated in hypertensive patients (Rabkin 2009). Furthermore, Gain-of-function mutations of the NLRP3 gene were reported to be associated with increased blood pressure in Finnish and Japanese populations (Omi et al. 2006, Kunnas et al. 2015). TLR4 expression is higher in circulating monocytes from patients with hypertension than in individuals without hypertension, and antihypertensive treatment downregulates its expression (Marketou et al. 2012). Monocytes from patients with essential hypertension are preactivated, producing greater amounts of IL-1β following *ex vivo* stimulation with Ang II or LPS

than monocytes from healthy controls (Dörffel et al. 1999). The clinical trial CANTOS showed marked benefits of IL-1β-targeted monoclonal antibody (canakinumab) therapy in patients with previous myocardial infarction in terms of reducing both circulating biomarkers of inflammation and cardiovascular events (Ridker et al. 2017). This opens up new avenues for immunotherapy in hypertension.

In the *in vitro* cellular model of this thesis, LPS acted via DAMPs to induce the formation of NLRP3 inflammasome in THP-1 cells. CRIP1 downregulation diminished the increase of inflammasome components after LPS stimulation. To further investigate the involvement of CRIP1 in this pathway, ATP was applied to activate the inflammasome via the P2X7 receptor (Bartlett et al. 2014). Subsequently, IL-1β and IL-18 protein release were measured in the supernatant, IL-1β and hopefully, IL-18 protein expression was also detected in cells.

As monocytes, shCRIP1 cells showed a low IL-1β basal release than shCtrl cells. Following NLRP3 inflammasome activation, IL-1β release from both shCtrl and shCRIP1 cells was significantly higher but not significantly different between the two groups. IL-1β expression was lower in shCRIP1 cells after NLRP3 inflammasome formation and activation. After being differentiated via PMA, less IL-1β was released from shCRIP1 cells to the supernatant after NLRP3 activation. Consistently, IL-1β expression was lower in shCRIP1 cells compared with shCtrl cells, also lower after NLRP3 inflammasome formation and activation (Figure 9).

IL-18 showed the same basal release in shCtrl and shCRIP1 monocytes, and it was significantly increased after LPS and ATP stimulation. Interestingly, after LPS induced NLRP3 formation, shCRIP1 cells released more IL-18, but after subsequently ATP induced NLRP3 activation, the releasement was particularly lower in shCRIP1 cells compared to shCtrl cells (Figure10).

Our results showed that CRIP1 downregulation avoids the activation of the NLRP3 inflammasome in monocytes and macrophages by decreased IL-1β and IL-18 protein content and secretion. This can also imply that CRIP1 can avoid hypertension and target organ damage by avoiding NLRP3 activation and reducing the production of associated inflammasome components, considering the role of these pro-inflammatory mediators in hypertension and CVDs. This provided new strategies for the early diagnosis and treatment of hypertension and CVDs. However, the effectiveness has to be further validated through animal studies and clinical trials.

The activation of NLRP3 inflammasome in our results was not directly detected but indirectly inferred from the activation of genes downstream of the signaling pathway. In future experiments, a specific inhibitor for NLRP3 will be applied to further confirm that this effect is NLRP3 inflammasome dependent.

The expression of IL-1β did not show great differences at the protein level consistent with the mRNA level, but they showed the same trend of change after stimulation. One of the supposed reasons may be an essential difference between mRNA and protein expression levels, considering the distinction of structure, functions, and

half-life of these molecules. Protein and mRNA correlations are not always predictable, studies that compared expression differences between these two molecules have found that the correlation between mRNA and protein levels was insufficient to predict protein expression levels from quantitative mRNA data (Gygi et al. 1999). However, a lot of research in this area has many technical limitations and it is often difficult to interpret why mRNA and protein levels correlate insignificantly. Another important factor in the differences between mRNA and protein abundance is the distinct synthesis and decay rates (Payne 2015).

Similarly, the intracellular expression levels of IL-1β did not correlate exactly with the levels released into the supernatant, which is easily explained by the fact that the IL-1β detected intracellularly was the unactivated pro-IL-1β, which remained regulated during the activation process, whereas the released activated IL-1β detected in the supernatant was the functional form.

In addition, after monocytes were differentiated via PMA, we observed no identical results. This is presumably because monocytes and differentiated macrophages are different cell types that have different biological functions and therefore differ in their response to inflammatory stimuli.

Figure 16 shows the proposed mechanism by which CRIP1 can interfere with the NLRP3 inflammasome signaling pathway in monocytes. CRIP1 may interact with NF-κB signaling and regulate its expression, thereby influencing NLRP3 inflammasome formation (signal 1) and downstream IL-1β/IL-18 activation, considering the effects observed in the induced inflammasome activation in the CRIP1 knockdown cell model, and further evidence that CRIP2, another member of the CRIP family, can also interact with NF-κB and mediate the transcriptional expression of related cytokines (Cheung et al. 2011).

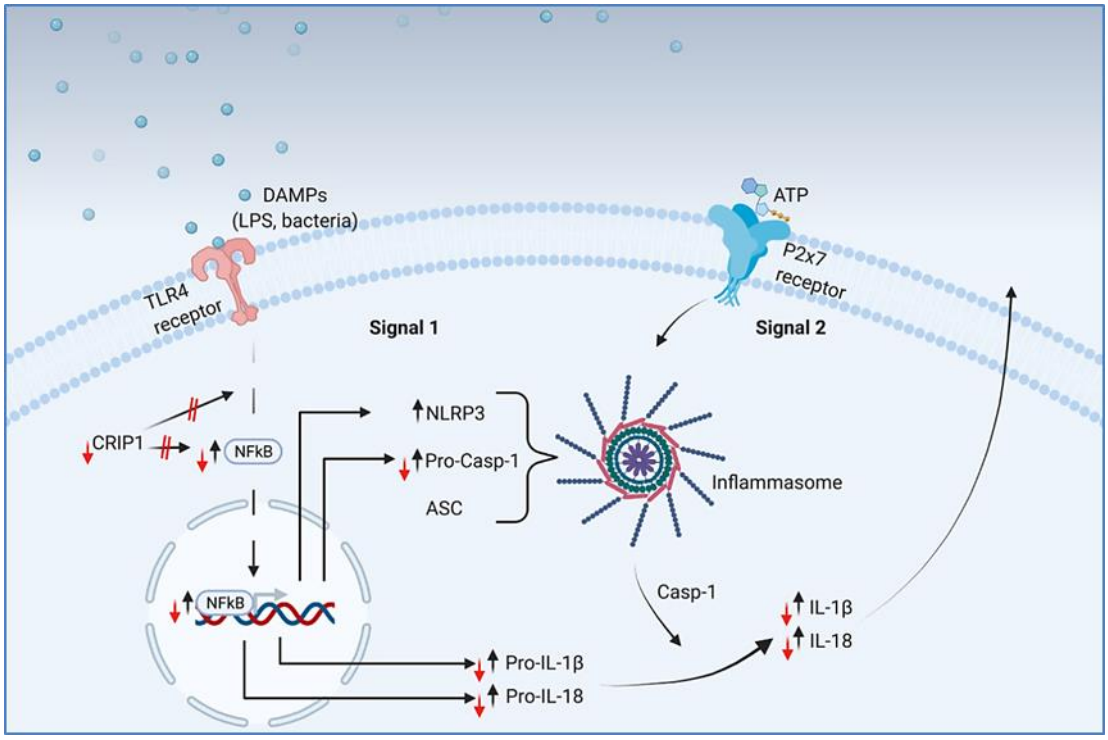


**Figure 16. A proposed mechanism for CRIP1 to regulate the NLRP3 inflammasome signaling pathway in monocytes (created with BioRender).** CRIP1 may interact with NF-κB signaling and regulate its expression, thereby influencing NLRP3 inflammasome formation and downstream IL-1β/IL-18 activation. Signal 1: Danger-associated molecular patterns (DAMPs) bind to Toll-like receptors (i.e. TLR4) and activate NF-κB leading to an upregulation of genes that control inflammasome components (i.e. NLRP3, Pro-Casp-1, Pro-IL-1β, Pro-IL-18). Signal 2: Activation of the inflammasome (i.e. ATP through P2x7 receptor) leads to cleavage of pro-Casp-1. Casp-1 catalyzes pro-IL-1β and pro-IL-18 to their active forms (IL-1β and IL-18). The active forms are released to the extracellular space and drive the inflammation. In red, the proposed mechanism by how downregulation of CRIP1 can affect NLRP3 inflammasome pathway.

### 4.1.2 CRIP1 influenced cell pyroptosis in monocytes

The NLRP3 inflammasome, in addition to IL-18 and IL-1β, not only plays pivotal roles in inflammation in cardiac and circulating inflammatory cells, but also in the occurrence of pyroptosis, caspase-1 dependent programmed cell death (Bergsbaken et al. 2009, Grundmann et al. 2011). Pyroptosis is a newly discovered form of cell death, which is driven by non-infectious factors, for example, host factors produced during MI (Bergsbaken et al. 2009). Unlike other programmed cell death, it was described as a strategy to maintain the inflammatory response through the release of pro-inflammatory intracellular contents during plasma membrane permeabilization. Studies have shown that cellular pyroptosis is widely involved in the development of atherosclerotic diseases and other diseases. The primary ischemic injury and the subsequent mitochondrial damage result in activation of the NLRP3 inflammasome in

the heart, inducing inflammatory cell pyroptosis in cardiomyocytes, further increasing myocardial injury and infarct size (Toldo et al. 2016, Toldo et al. 2015).

During activation of the NLRP3 inflammasome, Casp-1 cleaves gasdermin D and converts pro-IL-1β and pro-IL-18 to mature IL-1β and IL-18. Pyroptosis occurs through the insertion of the N-terminal fragment of gasdermin D into the plasma membrane, forming an oligomeric pore that allows the release of pro-inflammatory cytokines such as IL-1β and IL-18 into the extracellular space. The formation of pores also induces an influx of water into the cell, cell swelling and osmotic cell lysis, inducing further inflammation and hypertension by releasing more inflammatory products from the intracellular space (De Miguel et al. 2021).

In this thesis, cell viability and cytotoxicity were monitored in shCtrl and shCRIP1 cells. Cells exhibited similar cell viability profiles over a 72 hour monitoring period, while significant differences in cytotoxicity were observed from the 36-hour time point of monitoring, with shCRIP1 cells showing resistance against cytotoxicity after longer periods of seeding.

Combined with the previously described results that CRIP1 downregulation avoids the activation of the NLRP3 inflammasome by decreased IL-1β and IL-18 protein secretion, this result suggests a possible CRIP1 dependent regulation of cell pyroptosis. Thus, CRIP1 may be involved in the development of hypertension and end-organ damage by mediating cellular pyroptosis.

In this thesis, cell viability and cytotoxicity were monitored for only 72 hours due to limitations in the activity of the assay reagents, and therefore long-term results could not be obtained. In addition, we did not use pro- or anti-apoptotic reagents during our assay. This will be done in further experiments to reveal the regulatory role of CRIP1 in focal death.

### 4.1.3 CRIP1 altered other genes and inflammatory cytokines known to be involved in CVDs

Our results showed downregulation of *CRIP1* reduced *SH2B3* mRNA expression in THP1 cells. CRIP1 knockdown also weakened the overexpression of *CCL2* after induction of inflammation induced by LPS (Figure 7). This implied that CRIP1 participates in the regulation of SH2B3 and CCL2 expression, while both of them are widely known to be involved in the development of hypertension and CVDs.

The chemokine CCL2 (also known as MCP-1) activates monocytes and leukocytes by activating the CCR2 receptor and causing them to migrate to areas of inflammation. Production of CCL2 can be induced by Ang II and endothelin-1 (Funakoshi et al. 2001, Ishizawa et al. 2004), both important players in the development of hypertension and end-organ damage. Ang II receptor blockers reduce MCP-1 levels both in experimental models and in hypertension patient (Fliser et al. 2004). In addition, in animal models, genetic deletion of the MCP-1 axis or blockade of CCR2

lowers blood pressure and reduces vascular and renal inflammation (Shen et al. 2014, Chan et al. 2012). Pharmacological inhibition or genetic deficiency of CCR2 prevents the recruitment of monocytes and macrophages into the aortic wall and heart, limiting the development of hypertension and heart failure (Chan et al. 2012, Hulsmans et al. 2018, Moore et al. 2015). These findings highlight the therapeutic potential of inhibiting the CCL2 axis in the treatment of hypertension.

SH2B3 (also known as LNK) was identified in recent studies as a key driver gene for hypertension in humans, using a systems biology approach that integrates genomic data with whole blood transcriptomic data and network modeling (Levy et al. 2009, Newton-Cheh et al. 2009, Zeller et al. 2017). It was reported that in mice, hematopoietic SH2B3 deficiency leads to accelerated arterial thrombosis and atherosclerosis, in the setting of hypercholesterolemia (Wang et al. 2016). The mutation of *Sh2b3* may significantly attenuate Dahl salt-sensitive hypertension and renal disease (Rudemiller et al. 2015). The study of Saleh *et al.* (Saleh et al. 2015) described that deletion of Sh2b3 exacerbates Ang II-induced hypertension via mechanisms involving inflammation and T-cell activation. They determined that loss of SH2B3 exacerbates Ang II-induced hypertension and the associated renal and vascular dysfunction. Their results showed that, at baseline, kidneys from *Sh2b3*$^{-/-}$ mice exhibited greater levels of inflammation, oxidative stress, and glomerular injury compared with WT animals, and these parameters were further exacerbated by Ang II infusion. Aortas from *Sh2b3*$^{-/-}$ mice exhibited enhanced inflammation, reduced nitric oxide levels, and impaired endothelial-dependent relaxation.

Considering our result, we can speculate that the effect of *SH2B3* and *CCL2* on BP is mediated, at least in part by *CRIP1*. Although in this thesis, only the results of *in vitro* experiments at the cellular level are shown. In the future, generation of CRIP1 deficient mice will be applied to further underline the effect of CRIP1 on regulating SH2B3 and CCL2, thus contributing to hypertension and CVDs.

## 4.2 CRIP1 associated with inflammatory pathways in mice

The kidney is not only a major determinant of blood pressure but also a key target of inflammatory end-organ damage associated with hypertension. Inflammatory cells and their products contribute to blood pressure elevation at least in part by increasing renal sodium transport. Ultimately, uncontrolled inflammation results in renal fibrosis, oxidative stress, glomerular injury, and chronic kidney disease (Norlander et al. 2018).

Clinical and preclinical studies highlight a strong association between hypertension and conditions involving prolonged activation of the immune system, as well as certain infections such as with Porphyromonas gingivalis and cytomegalovirus (Czesnikiewicz‐Guzik et al. 2019, Hui et al. 2016). These observations suggest that chronic activation of the immune system by DAMPs and antigens not directly related to hypertension may, in some cases, have a spillover effect that promotes

inflammation and dysfunction within blood pressure-regulating organs (Drummond et al. 2019).

Recent literature suggests an important role for NLRP3 inflammasome in humans and animal models of kidney disease and hypertension. NLRP3 inflammasome involvement has been reported in glomerular and tubulointerstitial injury, where NLRP3 mRNA is significantly increased in renal biopsies of patients with various types of nondiabetic kidney disease, including acute tubular necrosis, focal segmental glomerulosclerosis, and hypertensive nephrosclerosis (Vilaysane et al. 2010). Many NLRP3 inflammasome components (NLRP3, ASC, Casp-1, IL-1β and IL-18) overexpressed in the kidney of spontaneously hypertensive rats (Krishnan et al. 2016). Studies have demonstrated that in mouse models of hypertension, protective effects of inflammasome inhibition in the two-kidney, one clip (2K1C) model, where NLRP3 or ASC deficiency prevents blood pressure elevation and lowers plasma renin activity (Wang et al. 2012). Additionally, in murine ATP-induced hypertension, ATP infusion resulted in increased salt-sensitive hypertension, caspase-1 activity, and IL-1β production in the renal medulla (Xia et al. 2012). Administration of caspase-1 inhibitor, however, blocked ATP-induced hypertension, reduced sodium retention, and blunted inflammasome activation and the production of IL-1β. Together, these data strongly implicate an important contribution of the NLRP3 inflammasome in the development of hypertension and related kidney disease.

In this thesis, the collaboration with the Institute for Immunology, University Medical Center Hamburg-Eppendorf, Prof. Hans-Willi Mittrücker allowed us to analyze the expression of *Crip1* and the inflammatory mediators of murine models for inflammation and kidney disease which were already published (Krebs et al. 2020) to verify the results observed in the *in vitro* part of this thesis.

### 4.2.1 CRIP1 associated with inflammatory pathways in the murine infection model

In the mouse infection model, kidneys showed the highest bacterial titers transiently by intravenous infection of mice with *S. aureus* than in other tissues, thus was used for further analysis in this thesis. Analysis of renal mRNA from this mouse infection model revealed that *Crip1* expression was upregulated at day 10 post-infection. At day 30 post-infection, mice were cleared of the bacteria by the immune response, or by anti-infective treatment with oral ampicillin. *Crip1* expression decreased to baseline levels in mice recovered from infection at day 30 (Figure 11). Similarly, *Nlrp3* mRNA expression was increased in *S. aureus* infected mice earlier from day 3 post-infection. In mice treated with oral ampicillin after infection, *Nlrp3* expression level returned to the same level as control mice at day 30 post-infection (Figure 12).

Compare to the regulation of *Crip1* during infection, *Nlrp3* was elevated earlier, and they both returned to basal level after anti-infective treatment with oral ampicillin. *Crip1* and *Nlrp3* showed similar trends of adjustment following infection, suggesting

the involvement of *Crip1* in the process of bacterially induced inflammatory responses and the possibility of an interaction with *Nlrp3*.

Inflammatory cytokines *Il-1β*, *Il-2*, *Il-6*, *Il-10*, and *Il-18* mRNA expression were also detected in kidney samples at day 3, 10, and 30 post-infection. The correlation between the expression of these cytokines and *Crip1* was analyzed (Figure 13). At day 10 post-infection, increased levels of *Crip1* expression were positively correlated with the high mRNA expression levels of pro-inflammatory cytokines. These inflammatory mediators have all been reported to be involved in the pathophysiological processes of hypertension and CVDs.

Pro-inflammatory cytokine IL-6 expression is elevated in hypertensive conditions (Bautista et al. 2005). Many studies have demonstrated that IL-6 is fundamental for the development of Ang II induced hypertension (Lee et al. 2006, Schrader et al. 2007, Brands et al. 2010). Studies by Brands *et al.* (Brands et al. 2010) found that activation of the JAK/STAT3 pathway by IL-6 plays a key role in the disease. Moreover, a human study further confirmed these results by showing that plasma levels of IL-6 increase in response to acute Ang II infusion and that these levels are exaggerated in hypertensive patients (Chamarthi et al. 2011). In more recent studies it has been shown that administration of IL-6 neutralizing antibody attenuated salt-sensitive hypertension, renal inflammation and injury in the salt-sensitive Dahl rat (Hashmat et al. 2016).

The up-regulation of *Il-17* in the kidney after the infection has been published in this model (Krebs et al. 2020). In recent years, the pro-inflammatory cytokine IL-17 has also been implicated in the development of hypertension. This cytokine is mainly produced by Th17 cells, macrophages, dendritic cells, and natural killer cells in response to immune activation (Wong et al. 2008). IL-17 was reported to be required for the maintenance of Ang II-induced hypertension and vascular dysfunction (Madhur et al. 2010). This effect of IL-17 on vascular function is mediated by promoting NOS3 phosphorylation, thus decreasing enzyme activity and NO production in endothelial cells (Nguyen et al. 2013). IL-17 could also be important in salt-sensitive hypertension, a recent study indicated that high salt may contribute to hypertension through mechanisms that trigger Th17 development and IL-17 production and promote tissue inflammation (Wu et al. 2013). Moreover, the vascular accumulation of leukocytes caused by Ang II is markedly reduced in IL-17$^{-/-}$ mice (Hartupee et al. 2007, Kao et al. 2005). Thus, IL-17 might contribute to the vascular pathophysiology of hypertension not only by direct effects, but also by recruiting other inflammatory cells to the perivascular tissue.

IL-2 is a pleiotropic cytokine with potent pro- and anti-inflammatory effects. IL-2 is a member of the type I family of cytokines. It is secreted by T cells activated by TCR-antigen presenting cell interactions. IL-2 drives the proliferation of effector T cells. IL-2 is a key player in the development of both effector T-cell and regulatory T-cell responses (De La Rosa et al. 2004). The administration of IL-2 to SHR (Tuttle

and Boppana 1990) and salt-sensitive Dahl rats (Ishimitsu et al. 1994) was found to ameliorate hypertension.

IL-10 is an important anti-inflammatory cytokine. Investigators have shown that Ang II increases vascular superoxide production in IL-$10^{-/-}$ mice, but not in wild-type animals (Didion et al. 2009). Administration of the anti-inflammatory cytokine IL-10 during pregnancy would attenuate hypertension, endothelial dysfunction, proteinuria, and inflammation seen in pregnant DOCA/saline-treated rats (Tinsley et al. 2010).

Together, these results implied that CRIP1 is involved in pathogen-induced inflammatory responses to kidney injury and subsequent possible hypertension development through complex interactions with NLRP3-related cytokines and other CVDs-related pro- and anti-inflammatory mediators. The biggest limitation in this model is that although CRIP1 expression was associated with NLRP3 and inflammatory mediators, we cannot determine the causal relationship between them.

Additionally, our results also showed that mRNA expression of markers known for leukocyte infiltration (*Adgre1, Ccl2 Cd44 Icam1* and *Itgam*) increased significantly from day 3 post *S.aureus* infection, and then gradually decreased as the infection recovered. This showed the same tendency as the regulation of CRIP1 during this process. The research results of Schweigert *et al.* (Schweigert et al. 2021) indicated that Ang II-induced migration of monocytes from the spleen to the blood was in a CRIP1-dependent manner. The released splenic monocytes may infiltrate organs in response to inflammatory processes that were caused by RAAS activation and hypertension. Our results also suggested that CRIP1 may be involved in the inflammatory process by regulating leukocyte infiltration.

### 4.2.2 CRIP1 associated with inflammatory pathways in the murine kidney disease model

An established experimental crescentic glomerulonephritis (cGN) model (Krebs et al. 2020, Kurts et al. 2013) was analyzed as another murine inflammation model. Upon induction of experimental glomerulonephritis, *Nlrp3, Il-1β, Il-2, Il-6, Il-10* and *Il-18* mRNA expression was increased in the renal cortex. *Crip1* mRNA expression was also increased and correlated to the elevated cytokines and *Nlrp3* expression, underlying CRIP1 participation in inflammasome activation.

The limitation is the same as the mouse infection model. We cannot determine the causal relationship of which step CRIP1 affects the activation of NLRP3. Thus, CRIP1 deficient mice will be needed in these models to further validate the hypothesis that the activation of the NLRP3 inflammasome pathway partly depends on CRIP1.

# 5. Limitations and Outlook

There are some limitations to this thesis.

Firstly, in the CRIP1 downregulated cell model, the activation of NLRP3 inflammasome was not directly detected but indirectly inferred from the activation of genes downstream of the signaling pathway, the exact mechanism of how CRIP1 acted is unclear. In future experiments, a specific inhibitor for NLRP3 will be applied to further confirm that this effect is NLRP3 inflammasome dependent. Parallelly, other inflammasome pathways such as NLRC4 will be excluded.

Secondly, the regulation of CRIP1 on the inflammasome pathway has only been elucidated through *in vitro* models, and in *ex vivo* murine inflammation models. CRIP1 expression was shown to be associated with NLRP3 and inflammatory markers, but we cannot determine the causal relationship between them. CRIP1 deficient mice will be needed in these models to further validate the hypothesis that the activation of NLRP3 partly depends on CRIP1 *in vivo*.

Despite the limitations, the results of this thesis provided a basis for a clearer view of CRIP1 function in relation to hypertension. CRIP1 is indicated to have the potential value as a biomarker for prognosis of CVDs and hypertension monitoring, also as a potential therapeutic target for inflammatory diseases. Further work will be done to underline these mechanisms and translate our findings of experimental models back to clinical application.

# 6. Summary

Hypertension is a complex polygenic disease and the exact underlying molecular mechanisms are yet to be understood. Hypertension increases the risk of CVD, stroke and renal failure. Inflammation has been identified as an essential process in the development of CVD such as myocardial infarction, ischemia/reperfusion and heart failure. Recently, in an interdisciplinary approach, expression of CRIP1 (cysteine-rich protein 1) was identified as being strongly associated with blood pressure. CRIP1 is highly expressed in immune cells like in monocytes, which suggests a correlation between CRIP1 and the pathophysiology of blood pressure through the immune system.

This thesis aimed to elucidate the role of CRIP1 on inflammation and CVD using a human monocytic cell line and murine inflammation models. In monocytic THP-1 cells, downregulation of CRIP1 via shRNA significantly altered the mRNA expression of cytokines known to be involved in CVD (*IL-1β*, *IL-18*, *CASP-1*, *NF-κB* and *CCL2*) after induction of inflammation by LPS. Furthermore, CRIP1 downregulation diminished the activation of the NLRP3 inflammasome by decreased IL-1β/IL-18 protein content and secretion suggesting a possible CRIP1- dependent regulation of pyroptosis.

Analysis of renal mRNA in murine *S.aureus* infection model revealed that *Crip1* was upregulated at day 10 and correlated the highest mRNA expression levels of proinflammatory cytokines. *Crip1* expression decreased in mice recovered from infection at day 30. Furthermore, *Crip1* expression correlated with the markers known for leukocyte infiltration during this process.

In an established experimental murine glomerulonephritis model, *Crip1* expression was upregulated in the kidney, which also correlated to the elevated proinflammatory cytokines and *Nlrp3* expression.

To summarize, our results indicated that CRIP1 participates in the regulation of inflammatory pathways, especially the NLRP3 inflammasome pathway in monocytes and kidneys. CRIP1 might contribute through these inflammation mechanisms to the development of hypertension considering the significance of inflammation in the progression of CVD.

This thesis adds to the understanding of the molecular basis of BP regulation, and CRIP1 is indicated to have the potential value as a CVD prognosis biomarker and therapeutic target. Generation of monocyte-specific and global CRIP1 deficient mice will be further worked to underline these results and translate our findings of experimental models back to clinical application. The results of this thesis provided a basis for a clearer view of CRIP1 function in relation to hypertension.

# Zusammenfassung

Hypertonie ist eine der bedeutenden Ursachen für Morbidität und Mortalität weltweit. Die Pathophysiologie des erhöhten Blutdrucks ist bis heute nicht vollständig geklärt. Zu den bekannten Risikofaktoren werden Lebensstil-, Umweltfaktoren, das Immunsystem und entzündliche Prozesse, sowie eine genetische Prädisposition, gezählt. Unkontrollierte Hypertonie erhöht das Risiko für kardiovaskulären Erkrankungen (CVD) wie Herzinfarkt, Herzinsuffizienz sowie das Risiko eines Nierenversagens. CRIP1 (cysteine-rich protein1) wurde bei einer Transkriptomanalyse humaner Monozyten als ein mögliches kardiovaskuläres Kandidatengen im Zusammenhang mit Bluthochdruck identifiziert. CRIP1 wird in Immunzellen wie Monozyten stark exprimiert, was auf einen Zusammenhang zwischen CRIP1 und der Pathophysiologie des Blutdrucks durch das Immunsystem hindeutet.

Ziel dieser Arbeit war es, den Beitrag von CRIP1 bei Entzündungen und CVD mittels einer humanen monozytären Zelllinie und murinen Entzündungsmodellen aufzuklären. In THP-1 Zellen führte die Herunterregulierung von CRIP1 mittels shRNA und nach Induktion einer Entzündung zu einer signifikanten Veränderung der mRNA Expression von Entzündungsmediatoren, von denen bekannt ist, dass sie an CVD beteiligt sind (*IL-1β*, *IL-18*, *CASP-1*, *NF-κB* und *CCL2*). Darüber hinaus verringerte die Herunterregulierung von CRIP1 die Aktivierung des NLRP3-Inflammasoms durch einen verringerten IL-1β/IL-18-Proteingehalt und eine geringere Sekretion, was auf eine mögliche CRIP1-abhängige Regulation der Pyroptose hindeutet.

Die Analyse der mRNA in der Niere von Mäusen, die mit *S. aureus* infiziert waren, ergab, dass *Crip1* am Tag 10 hochreguliert war und mit den höchsten mRNA-Expressionsniveaus proinflammatorischer Marker korrelierte. Die Expression von *Crip1* nahm bei Mäusen, die sich von der Infektion erholten, am Tag 30 ab. Darüber hinaus korrelierte die Expression von *Crip1* mit einer zunehmenden Leukozyteninfiltration während dieses Prozesses. In einem etablierten experimentellen Mausmodell für Glomerulonephritis war die Expression von *Crip1* in der Niere erhöht, was auch mit der erhöhten Expression von proinflammatorischen Zytokinen und *Nlrp3* korrelierte.

Zusammenfassend deuten unsere Ergebnisse darauf hin, dass CRIP1 an der Regulation von Entzündungswegen, insbesondere des NLRP3-Inflammasoms, in Monozyten und Nieren beteiligt ist. In Anbetracht der Bedeutung von Entzündungen für das Fortschreiten von CVD könnte CRIP1 über diese Entzündungsmechanismen zur Entwicklung von Bluthochdruck beitragen.

Diese Arbeit trägt zum molekularen Verständnis der Blutdruckregulation bei. CRIP1 könnte als Biomarker für die CVD-Prognose und als therapeutisches Ziel dienen. Monozytenspezifische und globale CRIP1-defiziente Mäuse werden benötigt, um diese Ergebnisse zu untermauern und unsere Erkenntnisse aus experimentellen Modellen in die klinische Anwendung zu übertragen.

# 7. List of Abbreviations

| Abbreviations | Full-form |
|---|---|
| µg | Microgram |
| µl | Microliter |
| ATP | Adenosine triphosphate |
| °C | Degree celcius |
| Ct | Cycle threshold |
| d | Days |
| h | Hours |
| $H_2O$ | Water |
| IL | Interleukin |
| kDa | kilo Dalton |
| LPS | Lipopolysaccharide |
| mg | Milligram |
| min | Minutes |
| ml | Milliliter |
| mM | Millimolar |
| ng | Nanogram |
| nM | Nanomolar |
| PBS | Phosphate-buffered saline |
| Pen / Strep | Penicillin / Streptomycin |
| pg | Picogram |
| PMA | Phorbol 12-myristate 13-acetate |
| rcf (g) | Relative centrifugal force |
| rpm | Rounds per minute |
| RT | Room temperature |
| s | Seconds |
| shCRIP1 | shRNA against CRIP1 |
| shCtrl | shRNA negative control |
| shRNA | Small / short hairpin RNA |
| V | Volt |

# 8. Reference

Aviv A and Lasker N (1992) Defects in membrane transport of ions as possible pathogenic factors in hypertension. Current opinion in nephrology and hypertension. 1(1): 68-72.

Avolio E, Pasqua T, Di Vito A, Fazzari G, Cardillo G, et al. (2018) Role of brain neuroinflammatory factors on hypertension in the spontaneously hypertensive rat. Neuroscience. 375: 158-168.

Bartlett R, Stokes L and Sluyter R (2014) The P2X7 receptor channel: recent developments and the use of P2X7 antagonists in models of disease. Pharmacological reviews. 66(3): 638-675.

Bautista LE, Vera LM, Arenas IA and Gamarra G (2005) Independent association between inflammatory markers (C-reactive protein, interleukin-6, and TNF-alpha) and essential hypertension. Journal of human hypertension. 19(2): 149-154.

Bell L and Madri JA (1990) Influence of the angiotensin system on endothelial and smooth muscle cell migration. The American journal of pathology. 137(1).

Bergsbaken T, Fink SL and Cookson BT (2009) Pyroptosis: host cell death and inflammation. Nature Reviews Microbiology. 7(2): 99-109.

Birkenmeier EH and Gordon JI (1986) Developmental regulation of a gene that encodes a cysteine-rich intestinal protein and maps near the murine immunoglobulin heavy chain locus. Proceedings of the National Academy of Sciences of the United States of America. 83(8): 2516-2520.

Bomfim GF, Dos Santos RA, Oliveira MA, Giachini FR, Akamine EH, et al. (2012) Toll-like receptor 4 contributes to blood pressure regulation and vascular contraction in spontaneously hypertensive rats. Clinical science (London, England : 1979). 122(11): 535-543.

Brands MW, Banes-Berceli AKL, Inscho EW, Al-Azawi H, Allen AJ, et al. (2010) Interleukin 6 knockout prevents angiotensin II hypertension: role of renal vasoconstriction and janus kinase 2/signal transducer and activator of transcription 3 activation. Hypertension (Dallas, Tex. : 1979). 56(5): 879-884.

Brunskill EW, Sequeira-Lopez MLS, Pentz ES, Lin E, Yu J, et al. (2011) Genes that confer the identity of the renin cell. Journal of the American Society of Nephrology : JASN. 22(12): 2213-2225.

Cai A and Calhoun DA (2017) Resistant Hypertension: An Update of Experimental and Clinical Findings. Hypertension (Dallas, Tex. : 1979). 70(1): 5-9.

Cai H, Chen J, Liu J, Zeng M, Ming F, et al. (2017) CRIP1, a novel immune-related protein, activated by Enterococcus faecalis in porcine gastrointestinal epithelial cells. Gene. 598: 84-96.

Castellanos-Rivera RM, Pentz ES, Lin E, Gross KW, Medrano S, et al. (2015) Recombination signal binding protein for Ig-κJ region regulates juxtaglomerular cell phenotype by activating the myo-endocrine program and suppressing ectopic gene expression. Journal of the American Society of Nephrology : JASN. 26(1): 67-80.

Chamarthi B, Williams GH, Ricchiuti V, Srikumar N, Hopkins PN, et al. (2011) Inflammation and hypertension: the interplay of interleukin-6, dietary sodium, and the renin-angiotensin system in humans. American journal of hypertension. 24(10): 1143-1148.

Chan CT, Moore JP, Budzyn K, Guida E, Diep H, et al. (2012) Reversal of vascular macrophage accumulation and hypertension by a CCR2 antagonist in deoxycorticosterone/salt-treated mice. Hypertension (Dallas, Tex. : 1979). 60(5): 1207-1212.

Chanput W, Mes J, Vreeburg RA, Savelkoul HF and Wichers HJ (2010) Transcription profiles of LPS-stimulated THP-1 monocytes and macrophages: a tool to study inflammation modulating effects of food-derived compounds. Food & function. 1(3): 254-261.

Chanput W, Mes JJ and Wichers HJ (2014) THP-1 cell line: an in vitro cell model for immune modulation approach. International immunopharmacology. 23(1): 37-45.

Cheung AKL, Ko JM, Lung HL, Chan KW, Stanbridge EJ, et al. (2011) Cysteine-rich intestinal protein 2 (CRIP2) acts as a repressor of NF-κB–mediated proangiogenic cytokine transcription to suppress tumorigenesis and angiogenesis. Proceedings of the National Academy of Sciences. 108(20): 8390-8395.

Chiong JR, Aronow WS, Khan IA, Nair CK, Vijayaraghavan K, et al. (2008) Secondary hypertension: current diagnosis and treatment. International journal of cardiology. 124(1): 6-21.

Chow CK, Teo KK, Rangarajan S, Islam S, Gupta R, et al. (2013) Prevalence, awareness, treatment, and control of hypertension in rural and urban communities in high-, middle-, and low-income countries. JAMA. 310(9): 959-968.

Czesnikiewicz‐Guzik M, Nosalski R, Mikolajczyk TP, Vidler F, Dohnal T, et al. (2019) Th1‐type immune responses toPorphyromonas gingivalisantigens exacerbate angiotensin II‐dependent hypertension and vascular dysfunction. British Journal of Pharmacology. 176(12): 1922-1931.

Dange RB, Agarwal D, Teruyama R and Francis J (2015) Toll-like receptor 4 inhibition within the paraventricular nucleus attenuates blood pressure and inflammatory response in a genetic model of hypertension. Journal of neuroinflammation. 12(1): 1-15.

De La Rosa M, Rutz S, Dorninger H and Scheffold A (2004) Interleukin‐2 is essential for CD4+ CD25+ regulatory T cell function. European journal of immunology. 34(9): 2480-2488.

De Miguel C, Pelegrín P, Baroja-Mazo A and Cuevas S (2021) Emerging Role of the Inflammasome and Pyroptosis in Hypertension. International Journal of Molecular Sciences. 22(3): 1064.

Didion SP, Kinzenbaw DA, Schrader LI, Chu Y and Faraci FM (2009) Endogenous interleukin-10 inhibits angiotensin II-induced vascular dysfunction. Hypertension (Dallas, Tex. : 1979). 54(3): 619-624.

Dörffel Y, Lätsch C, Stuhlmüller B, Schreiber S, Scholze S, et al. (1999) Preactivated peripheral blood monocytes in patients with essential hypertension. Hypertension (Dallas, Tex. : 1979). 34(1): 113-117.

Drummond GR, Vinh A, Guzik TJ and Sobey CG (2019) Immune mechanisms of hypertension. Nature reviews. Immunology. 19(8): 517-532.

Ehret GB, Ferreira T, Chasman DI, Jackson AU, Schmidt EM, et al. (2016) The genetics of blood pressure regulation and its target organs from association studies in 342,415 individuals. Nature genetics. 48(10): 1171-1184.

Ehret GB, Munroe PB, Rice KM, Bochud M, Johnson AD, et al. (2011) Genetic variants in novel pathways influence blood pressure and cardiovascular disease risk. Nature. 478(7367): 103-109.

Elliott EI and Sutterwala FS (2015) Initiation and perpetuation of NLRP3 inflammasome activation and assembly. Immunological reviews. 265(1): 35-52.

Escobar E (2002) Hypertension and coronary heart disease. Journal of human hypertension. 16(1): S61-S63.

Fanelli C, Arias SC, Machado FG, Okuma JK, Malheiros DM, et al. (2017) Innate and adaptive immunity are progressively activated in parallel with renal injury in the 5/6 renal ablation model. Scientific reports. 7(1): 1-15.

Fisher ND and Curfman G (2018) Hypertension—a public health challenge of global proportions. Jama. 320(17): 1757-1759.

Fliser D, Buchholz K and Haller H (2004) Antiinflammatory effects of angiotensin II subtype 1 receptor blockade in hypertensive patients with microinflammation. Circulation. 110(9): 1103-1107.

Folkow B, Johansson B and Mellander S (1961) The comparative effects of angiotensin and noradrenaline on consecutive vascular sections. Acta physiologica Scandinavica. 53.

Forouzanfar MH, Liu P, Roth GA, Ng M, Biryukov S, et al. (2017) Global Burden of Hypertension and Systolic Blood Pressure of at Least 110 to 115 mm Hg, 1990-2015. JAMA. 317(2): 165-182.

Frangogiannis NG (2014) The inflammatory response in myocardial injury, repair, and remodelling. Nature reviews. Cardiology. 11(5): 255-265.

Funakoshi Y, Ichiki T, Shimokawa H, Egashira K, Takeda K, et al. (2001) Rho-kinase mediates angiotensin II-induced monocyte chemoattractant protein-1 expression in rat vascular smooth muscle cells. Hypertension (Dallas, Tex. : 1979). 38(1): 100-104.

Gan W, Ren J, Li T, Lv S, Li C, et al. (2018) The SGK1 inhibitor EMD638683, prevents Angiotensin II–induced cardiac inflammation and fibrosis by blocking NLRP3 inflammasome activation. Biochimica et Biophysica Acta (BBA)-Molecular Basis of Disease. 1864(1): 1-10.

Gong W, Mao S, Yu J, Song J, Jia Z, et al. (2016) NLRP3 deletion protects against renal fibrosis and attenuates mitochondrial abnormality in mouse with 5/6 nephrectomy. American Journal of Physiology-Renal Physiology. 310(10): F1081-F1088.

Gottesman RF, Albert MS, Alonso A, Coker LH, Coresh J, et al. (2017) Associations Between Midlife Vascular Risk Factors and 25-Year Incident Dementia in the Atherosclerosis Risk in Communities (ARIC) Cohort. JAMA neurology. 74(10): 1246-1254.

Grahames C, Michel A, Chessell I and Humphrey P (1999) Pharmacological characterization of ATP‐and LPS‐induced IL‐1β release in human monocytes. British journal of pharmacology. 127(8): 1915-1921.

Grundmann S, Bode C and Moser M (2011). Inflammasome activation in reperfusion injury: friendly fire on myocardial infarction? : Am Heart Assoc.

Gygi SP, Rochon Y, Franza BR and Aebersold R (1999) Correlation between Protein and mRNA Abundance in Yeast. Molecular and Cellular Biology. 19(3): 1720-1730.

Hallquist NA, Khoo C and Cousins RJ (1996) Lipopolysaccharide regulates cysteine-rich intestinal protein, a zinc-finger protein, in immune cells and plasma. Journal of leukocyte biology. 59(2): 172-177.

Harrison DG, Vinh A, Lob H and Madhur MS (2010) Role of the adaptive immune system in hypertension. Current opinion in pharmacology. 10(2): 203-207.

Hartupee J, Liu C, Novotny M, Li X and Hamilton T (2007) IL-17 enhances chemokine gene expression through mRNA stabilization. Journal of immunology (Baltimore, Md. : 1950). 179(6): 4135-4141.

Hashmat S, Rudemiller N, Lund H, Abais-Battad JM, Van Why S, et al. (2016) Interleukin-6 inhibition attenuates hypertension and associated renal damage in Dahl salt-sensitive rats. American journal of physiology. Renal physiology. 311(3): F555-F561.

Huan T, Meng Q, Saleh MA, Norlander AE, Joehanes R, et al. (2015) Integrative network analysis reveals molecular mechanisms of blood pressure regulation. Molecular systems biology. 11(1): 799.

Huang Y, Ollikainen M, Sipilä P, Mustelin L, Wang X, et al. (2018) Genetic and Environmental Effects on Gene Expression Signatures of Blood Pressure: A Transcriptome-Wide Twin Study. Hypertension (Dallas, Tex. : 1979). 71(3): 457-464.

Hui J, Qu Y-Y, Tang N, Liu Y-M, Zhong H, et al. (2016) Association of cytomegalovirus infection with hypertension risk: a meta-analysis. Wiener klinische Wochenschrift. 128(15-16): 586-591.

Hulsmans M, Sager HB, Roh JD, Valero-Muñoz M, Houstis NE, et al. (2018) Cardiac macrophages promote diastolic dysfunction. The Journal of experimental medicine. 215(2): 423-440.

Iadecola C, Yaffe K, Biller J, Bratzke LC, Faraci FM, et al. (2016) Impact of Hypertension on Cognitive Function: A Scientific Statement From the American Heart Association. Hypertension (Dallas, Tex. : 1979). 68(6): e67-e94.

Ishimitsu T, Uehara Y, Numabe A, Tsukada H, Ogawa Y, et al. (1994) Antihypertensive effect of interleukin-2 in salt-sensitive Dahl rats. Hypertension (Dallas, Tex. : 1979). 23(1): 68-73.

Ishizawa K, Yoshizumi M, Tsuchiya K, Houchi H, Minakuchi K, et al. (2004) Dual effects of endothelin-1 (1-31): induction of mesangial cell migration and facilitation of monocyte recruitment through monocyte chemoattractant protein-1 production by mesangial cells. Hypertension research : official journal of the Japanese Society of Hypertension. 27(6): 433-440.

Itani HA, McMaster WG, Saleh MA, Nazarewicz RR, Mikolajczyk TP, et al. (2016) Activation of Human T Cells in Hypertension: Studies of Humanized Mice and Hypertensive Humans. Hypertension (Dallas, Tex. : 1979). 68(1): 123-132.

Ji X, Naito Y, Hirokawa G, Weng H, Hiura Y, et al. (2012) P2X 7 receptor antagonism attenuates the hypertension and renal injury in Dahl salt-sensitive rats. Hypertension Research. 35(2): 173-179.

Johnson JG and Hunt JC (1982). Hypertension secondary to renal parenchymal disease. *Hypertensive Cardiovascular Disease: Pathophysiology and Treatment.* : Springer.

Kadrmas JL and Beckerle MC (2004) The LIM domain: from the cytoskeleton to the nucleus. Nature reviews. Molecular cell biology. 5(11): 920-931.

Kao C-Y, Huang F, Chen Y, Thai P, Wachi S, et al. (2005) Up-regulation of CC chemokine ligand 20 expression in human airway epithelium by IL-17 through a JAK-independent but MEK/NF-kappaB-dependent signaling pathway. Journal of immunology (Baltimore, Md. : 1950). 175(10): 6676-6685.

Kearney PM, Whelton M, Reynolds K, Muntner P, Whelton PK, et al. (2005) Global burden of hypertension: analysis of worldwide data. Lancet (London, England). 365(9455): 217-223.

Kelly J, Mangos G, Williamson P and Whitworth J (1998) Cortisol and hypertension. Clinical and Experimental Pharmacology and Physiology. 25(S1): S51-S56.

Khoo C, Blanchard RK, Sullivan VK and Cousins RJ (1997) Human cysteine-rich intestinal protein: cDNA cloning and expression of recombinant protein and identification in human peripheral blood mononuclear cells. Protein expression and purification. 9(3): 379-387.

Khoo C and Cousins RJ (1994) Purification and properties of rat cysteine-rich intestinal protein. The Biochemical journal. 299 ( Pt 2): 445-450.

Krebs CF, Reimers D, Zhao Y, Paust H-J, Bartsch P, et al. (2020) Pathogen-induced tissue-resident memory T17 (T17) cells amplify autoimmune kidney disease. Science immunology. 5(50).

Krishnan S, Dowling J, Ling Y, Diep H, Chan C, et al. (2016) Inflammasome activity is essential for one kidney/deoxycorticosterone acetate/salt‐induced hypertension in mice. British journal of pharmacology. 173(4): 752-765.

Krishnan SM, Ling YH, Huuskes BM, Ferens DM, Saini N, et al. (2019) Pharmacological inhibition of the NLRP3 inflammasome reduces blood pressure, renal damage, and dysfunction in salt-sensitive hypertension. Cardiovascular research. 115(4): 776-787.

Krishnan SM, Sobey CG, Latz E, Mansell A and Drummond GR (2014) IL-1β and IL-18: inflammatory markers or mediators of hypertension? British journal of

pharmacology. 171(24): 5589-5602.

Kunnas T, Määttä K and Nikkari ST (2015) NLR family pyrin domain containing 3 (NLRP3) inflammasome gene polymorphism rs7512998 (C>T) predicts aging-related increase of blood pressure, the TAMRISK study. Immunity & ageing : I & A. 12: 19.

Kurts C, Panzer U, Anders H-J and Rees AJ (2013) The immune system and kidney disease: basic concepts and clinical implications. Nature reviews. Immunology. 13(10): 738-753.

Lanningham-Foster L, Green CL, Langkamp-Henken B, Davis BA, Nguyen KT, et al. (2002) Overexpression of CRIP in transgenic mice alters cytokine patterns and the immune response. American journal of physiology. Endocrinology and metabolism. 282(6): E1197-E1203.

Laragh J (1969) Renal and adrenal factors in hypertension: diagnostic approaches. Bulletin of the New York Academy of Medicine. 45(9): 859.

Latz E, Xiao TS and Stutz A (2013) Activation and regulation of the inflammasomes. Nature Reviews Immunology. 13(6): 397-411.

Lee DL, Sturgis LC, Labazi H, Osborne JB, Fleming C, et al. (2006) Angiotensin II hypertension is attenuated in interleukin-6 knockout mice. American journal of physiology. Heart and circulatory physiology. 290(3): H935-H940.

Levy D, DeStefano AL, Larson MG, O'Donnell CJ, Lifton RP, et al. (2000) Evidence for a gene influencing blood pressure on chromosome 17. Genome scan linkage results for longitudinal blood pressure phenotypes in subjects from the framingham heart study. Hypertension (Dallas, Tex. : 1979). 36(4): 477-483.

Levy D, Ehret GB, Rice K, Verwoert GC, Launer LJ, et al. (2009) Genome-wide association study of blood pressure and hypertension. Nature genetics. 41(6): 677-687.

Lewington S, Clarke R, Qizilbash N, Peto R and Collins R (2002) Age-specific relevance of usual blood pressure to vascular mortality: a meta-analysis of individual data for one million adults in 61 prospective studies. Lancet (London, England). 360(9349): 1903-1913.

Li EC, Heran BS and Wright JM (2014) Angiotensin converting enzyme (ACE) inhibitors versus angiotensin receptor blockers for primary hypertension. Cochrane Database of Systematic Reviews. (8).

Li P-L (2015). Cardiovascular pathobiology of inflammasomes: inflammatory machinery and beyond. : Mary Ann Liebert, Inc. 140 Huguenot Street, 3rd Floor New Rochelle, NY 10801 USA.

Lieb W, Jansen H, Loley C, Pencina MJ, Nelson CP, et al. (2013) Genetic predisposition to higher blood pressure increases coronary artery disease risk. Hypertension (Dallas, Tex. : 1979). 61(5).

Ling L, Chen D, Tong Y, Zang Y-H, Ren X-S, et al. (2018) Fibronectin type III domain containing 5 attenuates NLRP3 inflammasome activation and phenotypic transformation of adventitial fibroblasts in spontaneously hypertensive rats. Journal of hypertension. 36(5): 1104-1114.

Lip GYH, Coca A, Kahan T, Boriani G, Manolis AS, et al. (2017) Hypertension and

cardiac arrhythmias: executive summary of a consensus document from the European Heart Rhythm Association (EHRA) and ESC Council on Hypertension, endorsed by the Heart Rhythm Society (HRS), Asia-Pacific Heart Rhythm Society (APHRS), and Sociedad Latinoamericana de Estimulación Cardíaca y Electrofisiología (SOLEACE). European heart journal. Cardiovascular pharmacotherapy. 3(4): 235-250.

Llewellyn A, Simmonds M, Owen CG and Woolacott N (2016) Childhood obesity as a predictor of morbidity in adulthood: a systematic review and meta-analysis. Obesity reviews : an official journal of the International Association for the Study of Obesity. 17(1): 56-67.

Madhur MS, Lob HE, McCann LA, Iwakura Y, Blinder Y, et al. (2010) Interleukin 17 promotes angiotensin II-induced hypertension and vascular dysfunction. Hypertension (Dallas, Tex. : 1979). 55(2): 500-507.

Marketou ME, Kontaraki JE, Zacharis EA, Kochiadakis GE, Giaouzaki A, et al. (2012) TLR2 and TLR4 gene expression in peripheral monocytes in nondiabetic hypertensive patients: The effect of intensive blood pressure–lowering. The Journal of Clinical Hypertension. 14(5): 330-335.

Mathias CJ (1987) Role of the central nervous system in human secondary hypertension. Journal of cardiovascular pharmacology. 10: S93-9.

Mayet J and Hughes A (2003) Cardiac and vascular pathophysiology in hypertension. Heart. 89(9): 1104-1109.

Mazzali M, Hughes J, Kim YG, Jefferson JA, Kang DH, et al. (2001) Elevated uric acid increases blood pressure in the rat by a novel crystal-independent mechanism. Hypertension (Dallas, Tex. : 1979). 38(5): 1101-1106.

Mikolajczyk TP, Szczepaniak P, Vidler F, Maffia P, Graham GJ, et al. (2021) Role of inflammatory chemokines in hypertension. Pharmacology & therapeutics. 223: 107799.

Mills KT, Bundy JD, Kelly TN, Reed JE, Kearney PM, et al. (2016) Global Disparities of Hypertension Prevalence and Control: A Systematic Analysis of Population-Based Studies From 90 Countries. Circulation. 134(6): 441-450.

Mills KT, Stefanescu A and He J (2020) The global epidemiology of hypertension. Nature Reviews Nephrology. 16(4): 223-237.

Moore JP, Vinh A, Tuck KL, Sakkal S, Krishnan SM, et al. (2015) M2 macrophage accumulation in the aortic wall during angiotensin II infusion in mice is associated with fibrosis, elastin loss, and elevated blood pressure. American journal of physiology. Heart and circulatory physiology. 309(5): H906-H917.

Nakamura S, Kawai K, Takeshita Y, Honda M, Takamura T, et al. (2012) Identification of blood biomarkers of aging by transcript profiling of whole blood. Biochemical and biophysical research communications. 418(2): 313-318.

Nasution SA (2006) The use of ACE inhibitor in cardiovascular disease. Acta medica Indonesiana. 38(1): 60-64.

Newton-Cheh C, Johnson T, Gateva V, Tobin MD, Bochud M, et al. (2009) Genome-wide association study identifies eight loci associated with blood

pressure. Nature genetics. 41(6): 666-676.

Nguyen H, Chiasson VL, Chatterjee P, Kopriva SE, Young KJ, et al. (2013) Interleukin-17 causes Rho-kinase-mediated endothelial dysfunction and hypertension. Cardiovascular research. 97(4): 696-704.

Norlander AE, Madhur MS and Harrison DG (2018) The immunology of hypertension. J Exp Med. 215(1): 21-33.

Omi T, Kumada M, Kamesaki T, Okuda H, Munkhtulga L, et al. (2006) An intronic variable number of tandem repeat polymorphisms of the cold-induced autoinflammatory syndrome 1 (CIAS1) gene modifies gene expression and is associated with essential hypertension. European journal of human genetics : EJHG. 14(12): 1295-1305.

Palygin O, Levchenko V, Ilatovskaya DV, Pavlov TS, Ryan RP, et al. (2013) Real-time electrochemical detection of ATP and $H_2O_2$ release in freshly isolated kidneys. American journal of physiology. Renal physiology. 305(1): F134-F141.

Pasqua T, Pagliaro P, Rocca C, Angelone T and Penna C (2018) Role of NLRP-3 Inflammasome in Hypertension: A Potential Therapeutic Target. Curr Pharm Biotechnol. 19(9): 708-714.

Payne SH (2015) The utility of protein and mRNA correlation. Trends in biochemical sciences. 40(1): 1-3.

Prager P, Hollborn M, Steffen A, Wiedemann P, Kohen L, et al. (2016) P2Y1 Receptor Signaling Contributes to High Salt-Induced Priming of the NLRP3 Inflammasome in Retinal Pigment Epithelial Cells. PloS one. 11(10): e0165653.

Qi J, Yu X-J, Shi X-L, Gao H-L, Yi Q-Y, et al. (2016a) NF-κB blockade in hypothalamic paraventricular nucleus inhibits high-salt-induced hypertension through NLRP3 and caspase-1. Cardiovascular toxicology. 16(4): 345-354.

Qi J, Zhao X-F, Yu X-J, Yi Q-Y, Shi X-L, et al. (2016b) Targeting interleukin-1 beta to suppress sympathoexcitation in hypothalamic paraventricular nucleus in Dahl salt-sensitive hypertensive rats. Cardiovascular toxicology. 16(3): 298-306.

Rabkin SW (2009) The role of interleukin 18 in the pathogenesis of hypertension-induced vascular disease. Nature Reviews Cardiology. 6(3): 192-199.

Raj M (2011) Essential hypertension in adolescents and children: Recent advances in causative mechanisms. Indian journal of endocrinology and metabolism. 15 Suppl 4: S367-S373.

Ren X-S, Tong Y, Ling L, Chen D, Sun H-J, et al. (2017) NLRP3 gene deletion attenuates angiotensin II-induced phenotypic transformation of vascular smooth muscle cells and vascular remodeling. Cellular Physiology and Biochemistry. 44(6): 2269-2280.

Ridker PM, Everett BM, Thuren T, MacFadyen JG, Chang WH, et al. (2017) Antiinflammatory Therapy with Canakinumab for Atherosclerotic Disease. The New England journal of medicine. 377(12): 1119-1131.

Rodr ǵuez-Iturbe B, Ferrebuz A, Vanegas V, Quiroz Y, Mezzano S, et al. (2005) Early

and sustained inhibition of nuclear factor-κB prevents hypertension in spontaneously hypertensive rats. Journal of Pharmacology and Experimental Therapeutics. 315(1): 51-57.

Rossier BC, Bochud M and Devuyst O (2017) The Hypertension Pandemic: An Evolutionary Perspective. Physiology (Bethesda, Md.). 32(2): 112-125.

Rotival M, Zeller T, Wild PS, Maouche S, Szymczak S, et al. (2011) Integrating genome-wide genetic variations and monocyte expression data reveals trans-regulated gene modules in humans. PLoS genetics. 7(12): e1002367.

Rovio SP, Pahkala K, Nevalainen J, Juonala M, Salo P, et al. (2017) Cardiovascular Risk Factors From Childhood and Midlife Cognitive Performance: The Young Finns Study. Journal of the American College of Cardiology. 69(18): 2279-2289.

Rudemiller NP, Lund H, Priestley JR, Endres BT, Prokop JW, et al. (2015) Mutation of SH2B3 (LNK), a genome-wide association study candidate for hypertension, attenuates Dahl salt-sensitive hypertension via inflammatory modulation. Hypertension. 65(5): 1111-1117.

Saleh MA, McMaster WG, Wu J, Norlander AE, Funt SA, et al. (2015) Lymphocyte adaptor protein LNK deficiency exacerbates hypertension and end-organ inflammation. The Journal of clinical investigation. 125(3): 1189-1202.

Saxena T, Ali AO and Saxena M (2018) Pathophysiology of essential hypertension: an update. Expert review of cardiovascular therapy. 16(12): 879-887.

Schmeichel KL and Beckerle MC (1994) The LIM domain is a modular protein-binding interface. Cell. 79(2): 211-219.

Schrader LI, Kinzenbaw DA, Johnson AW, Faraci FM and Didion SP (2007) IL-6 deficiency protects against angiotensin II induced endothelial dysfunction and hypertrophy. Arteriosclerosis, thrombosis, and vascular biology. 27(12): 2576-2581.

Schroder K and Tschopp J (2010) The inflammasomes. cell. 140(6): 821-832.

Schweigert O, Adler J, Langst N, Aissi D, Duque Escobar J, et al. (2021) CRIP1 expression in monocytes related to hypertension. Clin Sci (Lond). 135(7): 911-924.

Shen JZ, Morgan J, Tesch GH, Fuller PJ and Young MJ (2014) CCL2-dependent macrophage recruitment is critical for mineralocorticoid receptor-mediated cardiac fibrosis, inflammation, and blood pressure responses in male mice. Endocrinology. 155(3): 1057-1066.

Smith Pe, Krohn RI, Hermanson GT, Mallia AK, Gartner FH, et al. (1985) Measurement of protein using bicinchoninic acid. Analytical biochemistry. 150(1): 76-85.

Stamler J, Stamler R and Neaton JD (1993) Blood pressure, systolic and diastolic, and cardiovascular risks: US population data. Archives of internal medicine. 153(5): 598-615.

Straubinger J, Boldt K, Kuret A, Deng L, Krattenmacher D, et al. (2017) Amplified pathogenic actions of angiotensin II in cysteine-rich LIM-only protein 4-negative mouse hearts. FASEB journal : official publication of the

Federation of American Societies for Experimental Biology. 31(4): 1620-1638.

Sun H-J, Ren X-S, Xiong X-Q, Chen Y-Z, Zhao M-X, et al. (2017) NLRP3 inflammasome activation contributes to VSMC phenotypic transformation and proliferation in hypertension. Cell death & disease. 8(10): e3074-e3074.

Surendran P, Drenos F, Young R, Warren H, Cook JP, et al. (2016) Trans-ancestry meta-analyses identify rare and common variants associated with blood pressure and hypertension. Nature genetics. 48(10): 1151-1161.

Sutterwala FS, Ogura Y, Zamboni DS, Roy CR and Flavell RA (2006) NALP3: a key player in caspase-1 activation. Journal of Endotoxin Research. 12(4): 251-256.

Tinsley JH, South S, Chiasson VL and Mitchell BM (2010) Interleukin-10 reduces inflammation, endothelial dysfunction, and blood pressure in hypertensive pregnant rats. American journal of physiology. Regulatory, integrative and comparative physiology. 298(3): R713-R719.

Toldo S, Marchetti C, Mauro AG, Chojnacki J, Mezzaroma E, et al. (2016) Inhibition of the NLRP3 inflammasome limits the inflammatory injury following myocardial ischemia–reperfusion in the mouse. International Journal of Cardiology. 209: 215-220.

Toldo S, Mezzaroma E, Mauro AG, Salloum F, Van Tassell BW, et al. (2015) The inflammasome in myocardial injury and cardiac remodeling. Antioxidants & redox signaling. 22(13): 1146-1161.

Tsuchiya S, Yamabe M, Yamaguchi Y, Kobayashi Y, Konno T, et al. (1980) Establishment and characterization of a human acute monocytic leukemia cell line (THP‐1). International journal of cancer. 26(2): 171-176.

Tuttle RS and Boppana DP (1990) Antihypertensive effect of interleukin-2. Hypertension (Dallas, Tex. : 1979). 15(1): 89-94.

Van de Veerdonk FL, Netea MG, Dinarello CA and Joosten LA (2011) Inflammasome activation and IL-1β and IL-18 processing during infection. Trends in immunology. 32(3): 110-116.

Verhoeckx K, Cotter P, López-Expósito I, Kleiveland C, Lea T, et al. (2015) The impact of food bioactives on health: in vitro and ex vivo models. : .

Vilaysane A, Chun J, Seamone ME, Wang W, Chin R, et al. (2010) The NLRP3 inflammasome promotes renal inflammation and contributes to CKD. Journal of the American Society of Nephrology : JASN. 21(10): 1732-1744.

Wang Q, So A, Nussberger J, Ives A, Bagnoud N, et al. (2014) Renin-dependent hypertension in mice requires the NLRP3-inflammasome. J Hypertens. 3(187): 2167-1095.10001.

Wang Q, So A, Nussberger J, Tschopp J and Burnier M (2012) Impact of NLRP3 inflammasome on the development of hypertension and renal and cardiac hypertrophy in 2K1C and DOCA/salt mice. Kidney Research and Clinical Practice. 31(2): A83.

Wang W, Tang Y, Wang Y, Tascau L, Balcerek J, et al. (2016) LNK/SH2B3 loss of function promotes atherosclerosis and thrombosis. Circulation research. 119(6): e91-e103.

Warren HR, Evangelou E, Cabrera CP, Gao H, Ren M, et al. (2017) Genome-wide

association analysis identifies novel blood pressure loci and offers biological insights into cardiovascular risk. Nature genetics. 49(3): 403-415.

Whelton PK, Carey RM, Aronow WS, Casey DE, Collins KJ, et al. (2018) 2017 ACC/AHA/AAPA/ABC/ACPM/AGS/APhA/ASH/ASPC/NMA/PCNA Guideline for the Prevention, Detection, Evaluation, and Management of High Blood Pressure in Adults: Executive Summary: A Report of the American College of Cardiology/American Heart Association Task Force on Clinical Practice Guidelines. Hypertension (Dallas, Tex. : 1979). 71(6): 1269-1324.

Williams B, Mancia G, Spiering W, Agabiti Rosei E, Azizi M, et al. (2018) 2018 ESC/ESH Guidelines for the management of arterial hypertension. European heart journal. 39(33): 3021-3104.

Wong CK, Lit LCW, Tam LS, Li EKM, Wong PTY, et al. (2008) Hyperproduction of IL-23 and IL-17 in patients with systemic lupus erythematosus: implications for Th17-mediated inflammation in auto-immunity. Clinical immunology (Orlando, Fla.). 127(3): 385-393.

Wu C, Yosef N, Thalhamer T, Zhu C, Xiao S, et al. (2013) Induction of pathogenic TH17 cells by inducible salt-sensing kinase SGK1. Nature. 496(7446): 513-517.

Xia M, Xiong J, Boini K, Abais J and Li P-L (2012). Characteristics and hypertensive actions of renal medullary NALP3 inflammasomes in mice. : Wiley Online Library.

Zeller T, Schurmann C, Schramm K, Müller C, Kwon S, et al. (2017) Transcriptome-Wide Analysis Identifies Novel Associations With Blood Pressure. Hypertension (Dallas, Tex. : 1979). 70(4): 743-750.

Zhou B, Bentham J, Di Cesare M, Bixby H, Danaei G, et al. (2017) Worldwide trends in blood pressure from 1975 to 2015: a pooled analysis of 1479 population-based measurement studies with 19 · 1 million participants. The Lancet. 389(10064): 37-55.

Zhu Q, Li X-X, Wang W, Hu J, Li P-L, et al. (2016) Mesenchymal stem cell transplantation inhibited high salt-induced activation of the NLRP3 inflammasome in the renal medulla in Dahl S rats. American Journal of Physiology-Renal Physiology. 310(7): F621-F627.

Ziegler MG and Milic M (2017) Sympathetic nerves and hypertension in stress, sleep apnea, and caregiving. Current opinion in nephrology and hypertension. 26(1): 26-30.

Zuber SM, Kantorovich V and Pacak K (2011) Hypertension in pheochromocytoma: characteristics and treatment. Endocrinology and Metabolism Clinics. 40(2): 295-311.

# 9. Acknowledgments

Three years have passed and my time at the University of Hamburg is coming to an end. On the occasion of completing my thesis, I would like to thank everyone who has helped me.

First of all, I would like to thank my supervisor, Prof. Tanja Zeller, for her guidance and advice, which has helped me in my research. Prof. Tanja Zeller has been very helpful to me during the three years, in terms of study, practice and life. Her rigorous learning style, open-mindedness and tireless spirit have been of great benefit to me, and her serious and responsible attitude towards research has been a model for me to follow and will benefit me for the rest of my life.

Secondly, I would like to thank Dr. Jorge Duque Escobar and Dr. Olga Schweigert for their careful guidance and support during the design and implementation stages of the project, and for their tireless help in data checking and thesis revision, which enabled the project to proceed smoothly. I would like to express my sincere gratitude to them for their serious scientific attitude, rigorous academic spirit, and style of working for excellence, which has deeply influenced and inspired me.

In addition, I would like to express my sincere gratitude to my colleagues in the Molecular Cardiology Laboratory at UKE for their help in my studies and practice, and their concern for my life over the past three years. I am grateful to all the academics involved in this thesis for their research results, which have helped and inspired me. I would also like to thank my family for their support and understanding of my studies and work. In my future studies and workplace, I will persist in my diligent work style and practical research attitude, and strive to improve myself to repay all those who have helped and encouraged me!

# 10. Curriculum Vitae

Lebenslauf wurde aus datenschutzrechtlichen Gründen entfernt

# 11. Eidesstattliche Versicherung

Ich versichere ausdrücklich, dass ich die Arbeit selbständig und ohne fremde Hilfe verfasst, andere als die von mir angegebenen Quellen und Hilfsmittel nicht benutzt und die aus den benutzten Werken wörtlich oder inhaltlich entnommenen Stellen einzeln nach Ausgabe (Auflage und Jahr des Erscheinens), Band und Seite des benutzten Werkes kenntlich gemacht habe.

Ferner versichere ich, dass ich die Dissertation bisher nicht einem Fachvertreter an einer anderen Hochschule zur Überprüfung vorgelegt oder mich anderweitig um Zulassung zur Promotion beworben habe.

Ich erkläre mich einverstanden, dass meine Dissertation vom Dekanat der Medizinischen Fakultät mit einer gängigen Software zur Erkennung von Plagiaten überprüft werden kann.

Unterschrift: .....